

# A Mixing Model for Turbulent Reactive Flows based on Euclidean Minimum Spanning Trees

S. SUBRAMANIAM\* and S. B. POPE

*Sibley School of Mechanical and Aerospace Engineering, Cornell University, Ithaca, New York 14853-7501, USA*

In modeling turbulent reactive flows based on the transport equation for the joint probability density function (jpdf) of velocity and composition, the change in fluid composition due to convection and reaction is treated exactly, while molecular mixing has to be modeled. A new mixing model is proposed, which is local in composition space and which seeks to address problems encountered in flows with simultaneous mixing and reaction. In this model the change in particle composition is determined by particle interactions along the edges of a Euclidean minimum spanning tree (EMST) constructed in composition space. Results obtained for the model problem of passive scalars evolving under the influence of a mean scalar gradient in homogeneous turbulence are found to be in reasonable agreement with experimental findings of Sirivat and Warhaft (1983). The model is applied to the diffusion flame test model problem proposed by Norris and Pope (1991) and its performance is found to be superior to that of existing models. The essential feature of the new EMST mixing model, which accounts for its success in the diffusion flame test, is that mixing is modeled locally in composition space. © 1998 by The Combustion Institute

## NOMENCLATURE

<b>A</b>	acceleration	$\mathcal{T}$	inverse drift term
<b>B</b>	model coefficient	$u$	fluctuating velocity field, $u_j = U_j - \langle U_j \rangle$
<b>C</b>	convex region in composition space	$U, \mathbf{U}$	velocity
$C_\phi$	model constant	$\mathcal{U}$	uniformly distributed random variable
$C_{\beta\gamma}$	covariance matrix	<b>V</b>	sample space variable of $\mathbf{U}$
<b>D</b>	number of composition variables	$w$	importance weight
$\mathcal{D}$	diffusion coefficient in Langevin equation	$w_\nu$	edge-weight of $\nu^{\text{th}}$ edge
$f_{\mathbf{U}\phi}, f$	joint velocity–composition probability density function (pdf)	$W_\nu$	cumulative edge-weight of $\nu^{\text{th}}$ edge
<b>F</b>	cumulative distribution function (cdf) of composition	<b>x</b>	Cartesian vector in physical space
$F_Z$	cdf of particle age	<b>X</b>	mapping
<b>G</b>	standardized normal cdf	<b>X</b>	particle position
<b>H</b>	Heaviside function	<b>Y</b>	reaction progress variable
<b>I</b>	indicator function	$z$	sample space variable of $Z$
<b>k</b>	turbulent kinetic energy	<b>Z</b>	age property
<b>M, M</b>	interaction matrix	<b>Greek Symbols</b>	
<b>n</b>	decay exponent in grid turbulence	$\alpha$	model parameter controlling the variance decay rate
<b>N</b>	number of particles	$\Gamma$	composition diffusivity
<b>p</b>	probability, pressure	$\epsilon$	mean dissipation rate of turbulence
$R_\lambda$	Taylor-scale Reynolds number	$\eta$	sample space variable of Gaussian
<b>s</b>	scaled time	$\Theta$	mixing model term
<b>S</b>	reaction rate	$\lambda$	matrix eigenvalue
<b>t</b>	time	$\nu$	edge index
<b>T, T</b>	transformation matrix	$\xi$	mixture fraction
		$\Pi$	mixing model matrix
		$\rho$	scalar–velocity correlation
		$\Sigma$	variance function

\*Corresponding author. Address: T-3, M.S. B216, Los Alamos National Laboratory, Los Alamos, NM 87545.

$\tau$	time-scale, turbulence time-scale
$\varphi$	fluctuating composition field, $\varphi_\beta = \Phi_\beta - \langle \Phi_\beta \rangle$
$\phi, \phi, \Phi$	composition
$\phi'$	fluctuating composition
$\chi_{\beta\gamma}$	joint-dissipation tensor
$\psi$	sample space variable of $\phi$
$\Omega$	particle exchange coefficient
$\langle \omega \rangle$	mean turbulent frequency

### Subscripts

$0$	initial condition, state 0
$1$	state 1
MC	mapping closure quantity
$T$	quantity associated with the tree
$i, j, m, n$	particle index in ensemble, index of Cartesian coordinate
$I$	corresponding to the IEM model
$k$	index of Cartesian coordinate
$l$	lean, lower value of interval
$r$	rich
$s$	stoichiometric
$ss$	statistically stationary value
$u$	upper value of interval
$w$	width of interval
$\beta$	index of composition variable
$\nu$	edge index
$\phi$	quantity associated with composition

### Superscripts

$i$	particle index in ensemble
$\beta$	index of composition variable
*	transformed quantity
'	fluctuating quantity, standard deviation thereof

## INTRODUCTION

In turbulent reacting flows the fluid composition field at any given physical location changes due to convection, molecular mixing, and reaction. Probability density function (pdf) formulations are particularly suitable for the modeling of turbulent combustion problems since the effects of reaction and convection are in closed form [1]. Furthermore, in turbulent combustion, where the reaction rate exhibits a highly nonlinear dependence on temperature, the pdf ap-

proach is capable of predicting important extinction phenomena more accurately than moment closures which rely on questionable closure assumptions for the mean reaction rate. Pdf calculations of piloted jet diffusion flames [2] show good agreement with experimental measurements. In spite of the success of pdf methods in predicting phenomena such as extinction [2], studies [3] have revealed serious deficiencies in the modeling of the molecular mixing term in particular circumstances. The objective of this paper is to develop an improved mixing model which describes the mixing of an arbitrary number of reactive scalars in inhomogeneous flows.

Modeling mixing in pdf methods involves prescribing the evolution of stochastic particles in composition space such that they mimic the change in the composition of a fluid particle due to mixing in a turbulent flow. In addition to the closure and realizability problems common to all turbulence modeling, there are issues such as localness (described later in this section) which are specific to modeling mixing. Some of the difficulties inherent in developing a mixing model for multiple reactive scalars are now described.

The rate of scalar variance decay in high Reynolds number turbulence is controlled by the large scales. In the absence of a model for the scalar gradients or energy transfer in the scalar spectrum, it is reasonable to assume that the scalar variance decay rate is proportional to the mean turbulent frequency. The evolution of the scalar pdf, however, is determined by turbulent motions down to the smallest scales. Therefore, the scalar pdf evolution is difficult to model without explicit characterization of the small scales. Accounting for the effect of the small scales is also the natural way to include the effects of species diffusivity and differential diffusion. However, the description of these processes necessitates a higher level of closure and more computational expense.

Despite these observations, there is scope for improving mixing models without resorting to a higher level of closure. This is achieved by requiring mixing models to satisfy modeling principles that have a physical or mathematical basis. One principal drawback of many mixing models in current use (notably the interaction

by exchange with the mean (IEM) mixing model [4]) is that they are not local in composition space. In nonpremixed combustion with fast chemistry and initial equilibrium condition, the reaction is confined to reaction sheets and this drawback can result in the unphysical mixing of cold fuel and oxidizer across the reaction sheet as demonstrated by Norris and Pope [3] in a diffusion flame test problem. Such behavior is observed because the IEM (and other) mixing models violate the physics of mixing: namely, that it is the composition field in the neighborhood (in physical space) of a fluid particle that influences its mixing. Since the composition fields encountered in reality are smooth, this neighborhood in physical space corresponds to a neighborhood in composition space. It follows that if a mixing model is to perform satisfactorily in the diffusion flame test problem, which is representative of the coupling of reaction and mixing in nonpremixed combustion, then the model should reflect the fact that the change in composition due to mixing is influenced by the neighborhood in composition space. This motivates inclusion of a new principle which mixing models should satisfy, namely localness in composition space.

For any turbulent reactive flow there exists a region in composition space called the realizable region within which any point corresponds to a possible composition value that a fluid particle may attain. Points in composition space that lie outside the realizable region correspond to compositions that cannot occur and have no physical meaning (for instance, if the composition variables represent species mass fractions these may correspond to negative mass fractions or mass fractions greater than unity). Consequently mixing models should preserve the boundedness of compositions. The goal of this modeling effort is to provide a phenomenological description of mixing (without explicit representation of the physical processes associated with the small scales), while satisfying the important principles of boundedness and localness.

In this paper a new mixing model (referred to as the Euclidean minimum spanning tree [EMST] mixing model) that is local in composition space is described. This particle interaction mixing model is an extension of the map-

ping closure particle model to multiple scalars. For the purposes of validating the mixing model, an inert flow is first considered. The problem of scalar mixing under the influence of an imposed mean scalar gradient has been studied experimentally [5]. A model problem based on this flow is posed and results are presented. Comparisons are made with the experimental data and direct numerical simulations (DNS) data of Overholt and Pope [6]. The model performance in reactive flows is tested using the diffusion flame test model problem posed by Norris and Pope [3]. Results are compared with those obtained using the IEM mixing model. An earlier version of the EMST mixing model has also been applied to the piloted jet diffusion flame [7]. Qualitative results support the hypothesis that the model's localness property is responsible for an improved description of mixing at various axial locations in the flow field.

## MIXING MODELS

In this section the EMST mixing model is placed in the context of existing modeling efforts by first describing a class of mixing models to which it belongs. A list of performance criteria for mixing models is then presented. It is shown that the class of mixing models under consideration naturally satisfy some of these performance criteria.

In Monte Carlo simulations of inhomogeneous flows the solution domain in physical space is discretized into a number of cells for the purpose of extracting local mean quantities which appear in the particle evolution equations. Properties of particles drawn from the same cell are local in physical space. Furthermore, to a first approximation, the property fields in a cell can be assumed to be statistically homogeneous. Within each cell at any given time  $t$ , the joint pdf of velocity and composition is represented by an ensemble of  $N$  particles. If the number of compositions is  $D$ , let  $w_i$  represent the importance weight (such that the particle weights sum to unity) and  $\phi_{\beta i}$  ( $\beta = 1, \dots, D$ ) represent the composition of the  $i^{\text{th}}$  particle ( $i = 1, \dots, N$ ) at time  $t$ . Also let  $\mathbf{X}^{(i)}$  represent

the position and  $\mathbf{U}^{(i)}$  represent the velocity of the  $i^{\text{th}}$  particle.

The evolution equations of these particle properties can be written as:

$$\frac{d\mathbf{X}^{(i)}}{dt} = \mathbf{U}^{(i)} \quad (1)$$

$$\frac{d\mathbf{U}^{(i)}}{dt} = \mathbf{A}^{(i)} \quad (2)$$

$$\frac{d\phi_{\beta i}}{dt} = \Theta_{\beta}^{(i)} + S_{\beta}([\phi_i]), \quad (3)$$

where  $\mathbf{A}^{(i)}$  represents a model for the particle acceleration,  $\Theta_{\beta}$  represents the mixing model and  $S_{\beta}([\phi_i])$  represents the reaction rate of the  $\beta^{\text{th}}$  scalar, and  $[\phi_i]$  represents the vector of compositions corresponding to the location of the  $i^{\text{th}}$  particle in composition space. Each particle's position evolves according to its velocity and the velocity evolves by the model for particle acceleration. Mixing models describe the evolution of particle compositions in composition space which represent (in a stochastically equivalent sense) the composition change of a fluid particle under the effect of molecular mixing.

The evolution equation for the joint pdf of velocity and composition  $f_{\mathbf{U}\phi}(\mathbf{V}, \boldsymbol{\psi}; \mathbf{x}, t)$  (denoted  $f$  for brevity) implied by the particle equations is

$$\begin{aligned} \frac{\partial f}{\partial t} + V_j \frac{\partial f}{\partial x_j} = & - \frac{\partial}{\partial V_k} [\langle A_k | \mathbf{V}, \boldsymbol{\psi} \rangle f] \\ & - \frac{\partial}{\partial \psi_{\beta}} [\langle \Theta_{\beta} | \mathbf{V}, \boldsymbol{\psi} \rangle f] \\ & - \frac{\partial}{\partial \psi_{\beta}} [S_{\beta}([\boldsymbol{\psi}]) f]. \end{aligned} \quad (4)$$

### Particle Interaction Mixing Models

Particle interaction mixing models are characterized by

$$\Theta_{\beta}^{(i)} = - \frac{1}{w^{(i)}} M_{ij}^{(\beta)} \phi_{\beta j}. \quad (5)$$

The matrix  $M_{ij}^{(\beta)}$  represents the interaction between particles  $i$  and  $j$  for the  $\beta^{\text{th}}$  scalar (in practice the same matrix describes the interac-

tion for all the scalars but this is not required). Summation is implied over repeated indices unless they are in parentheses. Thus, in Eq. 5 there is summation over the suffix  $j$ , but not over  $i$ .

The specification of the interaction matrix coefficients cannot be arbitrary. In fact, several restrictions arise from principles that guide the modeling of mixing. It is useful to summarize a provisional list of these principles, which also serve as performance criteria on the basis of which the merit of different mixing models can be evaluated.

### Performance Criteria for Mixing Models

#### Conservation of Means

The exact evolution equations of the composition fields and their moments imply specific conditions that mixing models ( $\Theta_{\beta}$ ) must satisfy. For particle interaction mixing models this imposes conditions on the matrix interaction coefficients ( $M_{ij}$ ). In deriving these exact equations it is convenient to omit the terms due to reaction (since reaction is in closed form) though the mixing models themselves are valid for both inert and reactive flows.

Consider a set of  $D$  conserved, inert, passive composition fields,  $\Phi_{\beta}(\mathbf{x}, t)$ ,  $\beta = 1, \dots, D$ , each with the same diffusivity  $\Gamma$ , evolving from arbitrary initial conditions in constant density turbulence. Assuming Fickian diffusion, their evolution is described by:

$$\frac{\partial \Phi_{\beta}}{\partial t} + U_j \frac{\partial \Phi_{\beta}}{\partial x_j} = \Gamma \frac{\partial^2 \Phi_{\beta}}{\partial x_k \partial x_k}, \quad (6)$$

where  $U_j(\mathbf{x}, t)$  is the turbulent velocity field.

The evolution of the mean composition fields,  $\langle \Phi_{\beta} \rangle$ , is given by

$$\frac{\partial \langle \Phi_{\beta} \rangle}{\partial t} + \langle U_j \rangle \frac{\partial \langle \Phi_{\beta} \rangle}{\partial x_j} + \frac{\partial \langle u_j \phi_{\beta} \rangle}{\partial x_j} = \Gamma \frac{\partial^2 \langle \Phi_{\beta} \rangle}{\partial x_k \partial x_k}, \quad (7)$$

where  $\phi_{\beta} = \Phi_{\beta} - \langle \Phi_{\beta} \rangle$  and  $u_j = U_j - \langle U_j \rangle$ . The corresponding mean equation implied by the modeled pdf equation (Eq. 4) can also be derived. Multiplying Eq. 4 by  $\psi_{\beta}$  and integrating over the whole  $(\mathbf{V}, \boldsymbol{\psi})$  sample space results in the mean evolution equation

$$\frac{\partial \langle \phi_\beta \rangle}{\partial t} + \langle U_j \rangle \frac{\partial \langle \phi_\beta \rangle}{\partial x_j} + \frac{\partial \langle u_j \phi_\beta \rangle}{\partial x_j} = \langle \Theta_\beta \rangle. \quad (8)$$

In high Reynolds number turbulence, the term  $\Gamma \nabla^2 \langle \Phi_\beta \rangle$  is negligible compared to the other terms in Eq. 7 and can be omitted. This gives the requirement (Eq. 7, cf. Eq. 8)

$$\langle \Theta_\beta \rangle = 0. \quad (9)$$

From the above it is clear that the mixing model does not directly affect the mean scalar fields.

The implication of this requirement on the structure of the particle interaction matrix is now derived. The ensemble scalar mean is defined as

$$\langle \phi_\beta \rangle_N \equiv \sum_{i=1}^N w_i \phi_{\beta i}. \quad (10)$$

The evolution of the particle compositions (Eq. 5) assuming the same interaction matrix for all the compositions is

$$\frac{d\phi_{\beta i}}{dt} = -\frac{1}{w^{(i)}} \sum_{j=1}^N M_{ij} \phi_{\beta j}, \quad (11)$$

where the summation over other particles is explicitly written out. From these equations the evolution of the ensemble scalar mean can be written as:

$$\begin{aligned} \frac{d\langle \phi_\beta \rangle_N}{dt} &= -\sum_{i=1}^N \sum_{j=1}^N M_{ij} \phi_{\beta j} \\ &= -\sum_{j=1}^N \left\{ \sum_{i=1}^N M_{ij} \right\} \phi_{\beta j} \\ &= 0 \text{ if } \sum_{i=1}^N M_{ij} = 0. \end{aligned} \quad (12)$$

This special structure—namely that each column of  $M_{ij}$  sums to zero—automatically guarantees conservation of the ensemble scalar mean. The requirement  $\sum_{i=1}^N M_{ij} = 0$  is clearly a sufficient condition for conservation of the ensemble scalar mean. In fact, unless  $M_{ij}$  depends on  $\phi_{\beta j}$  in some contrived way, the derivation of Eq. 12 reveals that  $\sum_{i=1}^N M_{ij} = 0$  is also a *necessary* condition for conservation of the

ensemble scalar mean (since Eq. 12 cannot be satisfied by  $M_{ij}$  that violates this condition and is also independent of  $\phi_{\beta j}$ ).

### Decay of Variances

The exact evolution of the covariance of the composition fields,  $\langle \varphi_\beta \varphi_\gamma \rangle$  is

$$\begin{aligned} \frac{\partial \langle \varphi_\beta \varphi_\gamma \rangle}{\partial t} + \langle U_j \rangle \frac{\partial \langle \varphi_\beta \varphi_\gamma \rangle}{\partial x_j} + \frac{\partial \langle u_j \varphi_\beta \varphi_\gamma \rangle}{\partial x_j} \\ + \langle \varphi_\beta u_j \rangle \frac{\partial \langle \Phi_\gamma \rangle}{\partial x_j} + \langle \varphi_\gamma u_j \rangle \frac{\partial \langle \Phi_\beta \rangle}{\partial x_j} \\ = -\langle \chi_{\beta\gamma} \rangle + \Gamma \frac{\partial^2 \langle \varphi_\beta \varphi_\gamma \rangle}{\partial x_k \partial x_k}, \end{aligned} \quad (13)$$

where

$$\chi_{\beta\gamma} \equiv 2\Gamma \frac{\partial \varphi_\beta}{\partial x_k} \frac{\partial \varphi_\gamma}{\partial x_k},$$

and  $\langle \chi_{\beta\gamma} \rangle$  is the symmetric positive semidefinite “joint” dissipation tensor. The diagonal elements of this tensor are always non-negative and they cause the respective scalar variances to decay. In high Reynolds number turbulence the term  $\Gamma \nabla^2 \langle \varphi_\beta \varphi_\gamma \rangle$  is negligible compared to the other terms in Eq. 13 and can be omitted.

The corresponding scalar covariance equation implied by the modeled pdf equation is

$$\begin{aligned} \frac{\partial \langle \phi'_\beta \phi'_\gamma \rangle}{\partial t} + \langle U_j \rangle \frac{\partial \langle \phi'_\beta \phi'_\gamma \rangle}{\partial x_j} + \frac{\partial \langle u_j \phi'_\beta \phi'_\gamma \rangle}{\partial x_j} \\ + \langle \phi'_\beta u_j \rangle \frac{\partial \langle \phi_\gamma \rangle}{\partial x_j} + \langle \phi'_\gamma u_j \rangle \frac{\partial \langle \phi_\beta \rangle}{\partial x_j} \\ = \langle \phi'_\beta \Theta_\gamma \rangle + \langle \phi'_\gamma \Theta_\beta \rangle, \end{aligned} \quad (14)$$

where  $[\mathbf{u}^{(i)} = \mathbf{U}^{(i)} - \langle \mathbf{U} \rangle \langle \mathbf{X}^{(i)} \rangle]$  denotes the velocity fluctuations and  $[\phi'_i = \phi_i - \langle \phi \rangle \langle \mathbf{X}^{(i)} \rangle]$  represents the scalar fluctuations. Details of this derivation may be found in Ref. [8]. Comparing the terms in Eq. 14 with those in Eq. 13 it is clear that in the high Reynolds number limit  $\langle \chi_{\beta\gamma} \rangle^M \equiv -[\langle \phi'_\beta \Theta_\gamma \rangle + \langle \phi'_\gamma \Theta_\beta \rangle]$  is a model for  $\langle \chi_{\beta\gamma} \rangle$ .

From the properties of the “joint” dissipation tensor it follows that  $\langle \chi_{\beta\gamma} \rangle^M$  should also be a symmetric positive semidefinite tensor. In other words, for any vector  $x_\beta$  we require

$$\sum_{\beta} \sum_{\gamma} x_{\beta} x_{\gamma} \langle \chi_{\beta\gamma} \rangle^M \geq 0. \tag{15}$$

This in turn implies that the ensemble averaged counterpart of  $\langle \chi_{\beta\gamma} \rangle^M$ , which is defined as

$$\begin{aligned} \langle \chi_{\beta\gamma} \rangle_N^M &\equiv - \left[ \left\langle \phi'_{\beta} \frac{d\phi'_{\gamma}}{dt} \right\rangle_N + \left\langle \phi'_{\gamma} \frac{d\phi'_{\beta}}{dt} \right\rangle_N \right] \\ &= - \frac{d\langle \phi'_{\beta} \phi'_{\gamma} \rangle_N}{dt}, \end{aligned} \tag{16}$$

should also be positive semidefinite. For particle interaction models,  $\langle \chi_{\beta\gamma} \rangle_N^M$  can be expressed in terms of the interaction matrix  $\mathbf{M}$  as [8]:

$$\begin{aligned} \langle \chi_{\beta\gamma} \rangle_N^M &= \sum_{i=1}^N \sum_{j=1}^N M_{ij} (\phi'_{\gamma i} \phi'_{\beta j} + \phi'_{\beta i} \phi'_{\gamma j}) \\ &= \sum_{i=1}^N \sum_{j=1}^N (M_{ij} + M_{ji}) \phi'_{\beta i} \phi'_{\gamma j}. \end{aligned} \tag{17}$$

The second line in Eq. 17 follows simply by commuting  $i$  and  $j$  in the first term, i.e.

$$\begin{aligned} \sum_{i=1}^N \sum_{j=1}^N M_{ij} \phi'_{\gamma i} \phi'_{\beta j} &= \sum_{j=1}^N \sum_{i=1}^N M_{ji} \phi'_{\gamma j} \phi'_{\beta i} \\ &= \sum_{i=1}^N \sum_{j=1}^N M_{ji} \phi'_{\beta i} \phi'_{\gamma j}. \end{aligned}$$

Thus the condition in Eq. 15 can be written as:

$$\begin{aligned} \sum_{\beta} \sum_{\gamma} x_{\beta} x_{\gamma} \langle \chi_{\beta\gamma} \rangle_N^M &= \sum_{\beta} \sum_{\gamma} x_{\beta} x_{\gamma} \sum_{i=1}^N \sum_{j=1}^N (M_{ij} \\ &\quad + M_{ji}) \phi'_{\beta i} \phi'_{\gamma j} \\ &= \sum_{i=1}^N \sum_{j=1}^N (M_{ij} + M_{ji}) y_i y_j, \end{aligned}$$

where  $y_i \equiv \sum_{\beta} x_{\beta} \phi'_{\beta i}$ . The requirement for the decay of all variances is then:

$$\sum_{i=1}^N \sum_{j=1}^N (M_{ij} + M_{ji}) y_i y_j \geq 0,$$

which is satisfied for all  $\mathbf{x}$  (and therefore for all  $\mathbf{y}$ ), if and only if the symmetric part of  $\mathbf{M}$  ( $\mathbf{M}_s \equiv \frac{1}{2} [\mathbf{M} + \mathbf{M}^T]$ ) is positive semidefinite.

This mathematical condition is automatically

satisfied by *pairwise-exchange* mixing models, which are defined as having a symmetric interaction matrix with nonpositive off-diagonal elements:

$$M_{ij} = M_{ji} \leq 0 \quad \forall i \neq j,$$

and diagonal elements given by

$$\begin{aligned} M_{(i)(i)} &= - \sum_{j=1, j \neq i}^N M_{ij} \\ &= - \sum_{j=1, j \neq i}^N M_{ji}. \end{aligned}$$

This definition of the diagonal elements guarantees the conservation of the means (Eq. 12). In these models the interaction between the  $i^{th}$  and  $j^{th}$  particles is given by

$$w_{(i)} \frac{d\phi_{\beta i}}{dt} = -\Omega_{(i)(j)} (\phi_{\beta i} - \phi_{\beta j}),$$

and

$$w_{(j)} \frac{d\phi_{\beta j}}{dt} = -\Omega_{(i)(j)} (\phi_{\beta j} - \phi_{\beta i}),$$

where  $\Omega_{(i)(j)} = -M_{ij} \geq 0$ . Clearly this exchange conserves the mean (cf. Eq. 12) and decreases (or leaves unchanged) the difference  $|\phi_{\beta i} - \phi_{\beta j}|$  which contributes to the variance.

It follows from the Gershgorin circle theorem [9] (p. 341) that the eigenvalues  $\lambda(M)$  of  $M_{ij}$  lie in the interval

$$\begin{aligned} M_{(i)(i)} - \sum_{j=1, j \neq i}^N |M_{ij}| &\leq \lambda(M) \\ &\leq M_{(i)(i)} + \sum_{j=1, j \neq i}^N |M_{ij}| \end{aligned}$$

which is

$$0 \leq \lambda(M) \leq 2M_{(i)(i)},$$

and so indeed  $M_{ij}$  is positive semidefinite for pairwise-exchange models.

**Boundedness**

For every physical problem, a surface can be defined in composition space that is the bound-

ary of the region of realizable compositions. For nonreactive scalars with equal diffusivities, the composition values are restricted to an allowed region (a subset of the realizable region and dependent on the initial compositions), which is convex and decreases with time. The initial ensemble of particles with scalar properties  $\phi_{\beta i}(t = 0)$ ,  $i = 1, \dots, N$  is sampled from a specified initial jpdf and must lie in this allowed region. These particle locations define a convex hull in composition space which is denoted by  $C(0)$ . At later times the convex hull formed by  $\phi_{\beta i}(t)$  is denoted  $C(t)$ . It follows from the conservation equation (Eq. 6) that the convex hull can only shrink; i.e. for  $t_2 > t_1$ ,  $C(t_2) \subseteq C(t_1)$ . Boundedness is guaranteed if the evolution of particle properties is such that  $\phi_{\beta i}(t_2)$  lies in  $C(t_1)$ , thus ensuring  $C(t_2) \subseteq C(t_1)$ , for all  $t_1, t_2$  satisfying  $t_2 > t_1 \geq 0$ .

Any composition  $\hat{\phi}_\beta$  which can be expressed as a weighted sum of compositions, i.e.

$$\hat{\phi}_\beta = \theta_i \phi_{\beta i}(t), \quad i = 1, \dots, n \quad (18)$$

with  $\theta_i \geq 0$ ,  $\sum_{i=1}^n \theta_i = 1$ , lies within the convex hull  $C(t)$ .

Starting at any given time  $t$ , the particle compositions after an infinitesimal time interval  $dt$  evolving according to Eq. 11 can be written as

$$\begin{aligned} \phi_{\beta i}(t + dt) = & -\frac{dt}{w_{(i)}} \sum_{j=1, j \neq i}^N M_{i(j)} \phi_{\beta j}(t) + \left[ 1 \right. \\ & \left. - \frac{dt}{w_{(i)}} M_{(i)(i)} \right] \phi_{\beta i}(t). \end{aligned} \quad (19)$$

Using the fact that pairwise exchange models satisfy Eq. 12, Eq. 19 can be rewritten as

$$\begin{aligned} \phi_{\beta i}(t + dt) = & -\frac{dt}{w_{(i)}} \sum_{j=1, j \neq i}^N M_{i(j)} \phi_{\beta j}(t) + \left[ 1 \right. \\ & \left. + \frac{dt}{w_{(i)}} \sum_{j=1, j \neq i}^N M_{ij} \right] \phi_{\beta i}(t), \end{aligned}$$

where the right hand side is a weighted sum of the form in Eq. 18. In the first term, the coefficient  $-dtM_{i(j)}/w_{(i)}$  is a non-negative infinitesimal; and in the second term the coefficient of  $\phi_{\beta i}(t)$  is infinitesimally less than unity. Hence, every composition  $\phi_{\beta i}(t + dt)$  lies

within  $C(t)$ , and so  $C(t + dt) \subseteq C(t)$  thus establishing boundedness for pairwise-exchange models.

### Linearity and Independence

**Linearity.** The set of governing equations for the evolution of scalar fields in turbulence (Eq. 6) is linear with respect to the scalar fields. For equal diffusivities of all scalars, it follows that subjecting the set of scalars ( $\phi = \{\phi_\beta\}$ ,  $\beta = 1, \dots, D$ ) under consideration to an arbitrary linear transformation  $\mathbf{T}$  (which may be singular), such that

$$\phi_\gamma^* = T_{\gamma\beta} \phi_\beta, \quad (20)$$

results in the same set of governing equations for the transformed set of scalars ( $\phi^*$ ) [10]. The implication of this for particle models of multi-scalar mixing is that the evolution equation for particle properties of the scalars (including all model constants) should transform unchanged when the scalars are subject to an arbitrary linear transformation. For moment models the implication is that the models should only contain those statistics that transform linearly under linear transformations of the scalar set. For the case of unequal diffusivities the linear transformation is restricted to diagonal stretchings of the scalar fields. One of the implications of this principle is that there is no intrinsic set of scales in composition space for the set of scalars.

**Independence.** If we consider the mixing of a set of  $D$  conserved passive scalars denoted by  $\{\phi_\beta\}$ ,  $\beta = 1, \dots, D$ , then the evolution of any one of these scalar fields, say  $\phi_\beta(\mathbf{x}, t)$ , is unaffected by any of the other scalar fields  $\phi_\gamma$  ( $\gamma \neq \beta$ ). This is the independence principle proposed by Pope [10]. The implication of this for particle models of multiscalar mixing is that the evolution of the particle property of one scalar  $\phi_\beta$  should not depend on the particle properties or statistics of any of the other scalars  $\phi_\gamma$  ( $\gamma \neq \beta$ ). For moment models of multiscalar mixing, the implication is that the evolution of any statistic involving one scalar  $\phi_\beta$  should not depend on statistics involving any of the other scalars  $\phi_\gamma$  ( $\gamma \neq \beta$ ).

It may be noted that contrary to earlier notions, independence is a more fundamental condition that must be satisfied for the linearity

principle to hold. To illustrate this point, consider the class of mixing models represented by

$$\Theta_{\beta} = \Pi_{\beta\gamma}\phi_{\gamma} \quad (21)$$

which includes all particle interaction models (Eq. 5). While this is not the most general representation of a mixing model, it includes a majority of mixing models in current use barring those that have a diffusion term. Models that have nonzero off-diagonal entries in the matrix  $\Pi$  violate the independence principle. The corresponding model for the set of scalars obtained by the transformation given by Eq. 20 is

$$\Theta_{\beta}^* = \Pi_{\beta\gamma}\phi_{\gamma}^* \quad (22)$$

Noting that the transformation law requires that

$$\frac{d\phi^*}{dt} = \mathbf{T} \frac{d\phi}{dt} = \mathbf{T}\Pi\phi \quad (23)$$

and also

$$\frac{d\phi^*}{dt} = \Theta^* = \Pi\mathbf{T}\phi,$$

it is evident that the linearity principle requires

$$\Pi\mathbf{T} = \mathbf{T}\Pi, \quad (24)$$

for any  $\mathbf{T}$ . Any model  $\Pi$  with only diagonal entries (satisfying the independence principle) automatically satisfies the linearity condition expressed in Eq. 24. It is also easy to see that the condition is not satisfied by all nondiagonal matrices. This demonstrates that for mixing models expressible in the form of Eq. 21, independence is a necessary and sufficient condition for linearity. It is also noteworthy that for the case of unequal diffusivities the linearity condition is restricted to diagonal (stretching) transformations ( $\mathbf{T}$ ). In this situation there could be models of the form of Eq. 21 that violate independence but satisfy the linearity condition (Eq. 24) and here independence is sufficient but not necessary to satisfy linearity.

### Relaxation to Gaussian

In homogeneous isotropic turbulence, both experiments [11] and direct numerical simulations [12] indicate that the scalar pdf relaxes to a Gaussian after sufficient time has elapsed for

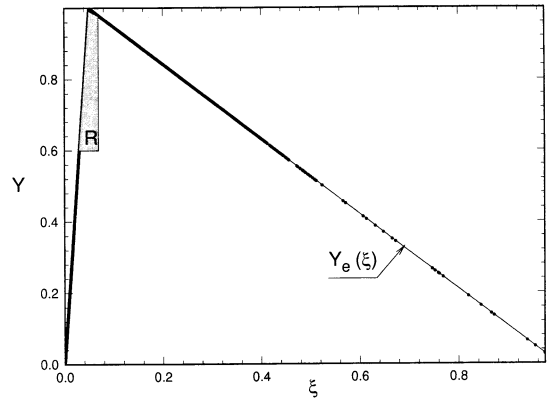


Fig. 1. Initial condition for the diffusion flame test: mixture fraction  $\xi$  is distributed according to a  $\beta$ -pdf with mean 0.1 and variance 0.01; progress variable  $Y$  is initially at equilibrium  $Y_e(\xi)$ ; thermochemistry is infinitely fast in the reaction zone  $R$  which is centered at the stoichiometric mixture fraction ( $\xi_s = 0.05$ ) and extends from  $\xi_l = 0.03$  to  $\xi_r = 0.07$ .

the solution to become independent of the initial conditions. It is desirable that a mixing model reproduce this behavior, though it is well known that this is not a necessary condition for satisfactory performance of the model in inhomogeneous flows.

### Localness

The concept of localness was motivated by the diffusion flame test which is now described. Consider an idealized diffusion flame in homogeneous isotropic turbulence with infinitely fast chemistry. The fluid composition is represented by two variables: mixture fraction  $\xi$  and a reaction progress variable  $Y$ . The initial condition for mixture fraction is chosen to be a  $\beta$ -distribution with mean (0.1) and variance (0.01) which correspond to a typical experiment. The progress variable is initially at equilibrium denoted by  $Y_e(\xi)$ . The one-step, irreversible reaction is confined to a region  $R$  in composition space as shown in Fig. 1. The region  $R$  is centered at the stoichiometric mixture fraction ( $\xi_s = 0.05$ ) and extends from the lean mixture fraction limit of  $\xi_l = 0.03$  to the rich mixture fraction limit of  $\xi_r = 0.07$ , for  $Y > 0.6$ .

As the flow evolves from this homogeneous initial condition, reactants enter the reaction zone by mixing and are instantly reacted to form products resulting in flame sheet combustion

[3]. The correct behavior expected of mixing models in this test is that the compositions remain along the equilibrium line for all time. For satisfactory behavior in this limit, a mixing model must be local in composition space. For particle interaction models this means that particles should mix with other particles in their immediate neighborhood in composition space. The reason for the failure of mixing models in the diffusion flame test is that they are not local in composition space, resulting in mixing of particles across the reaction zone.

The principle of localness can also be related to the structure of the interaction matrix for the case of a single scalar. Let the ensemble of  $N$  particles be ordered by nondecreasing scalar value such that

$$\phi_1 \leq \phi_2 \leq \dots \leq \phi_N,$$

where the  $\beta$  subscript indicating scalar dimension has been dropped since the composition space is one-dimensional. Since proximity in composition space of particle  $i$  to particle  $j$  (and hence, localness) is directly related to the difference between their indices, it follows that the bandwidth of the interaction matrix determines the localness of the particle interaction mixing model. The relation between localness and simple ordering holds only in a one-dimensional composition space.

### Dependence on Re

The effect of flow Reynolds number (for sufficiently large Reynolds number) on scalar mixing is to change the scalar spectra in the range of wavenumbers greater than those corresponding to the inertial subrange. While including a dependence on Reynolds number in the mixing model allows for a better description of mixing, this does not seem appropriate at the current level of closure.

### Differential Diffusion

When modeling practical combustion problems with different chemical species which may have different diffusivities (e.g.,  $H_2$  and  $N_2$  in hydrocarbon-air flames), it is desirable that the mixing model take these effects into account. This

requires modeling the effect of the small scales of turbulence.

### Dependence of Length Scales of Scalar Fields

Experiments of Warhaft and Lumley [13] show that the variance decay rate of a single conserved passive scalar in grid turbulence shows dependence on the initial length scales of the scalar field. The dependence of scalar mixing on the initial lengthscales of the scalar field has also been studied using direct numerical simulations of turbulent mixing of single [12] and multiple scalars [14]. The important conclusion from these sources is that the smaller the initial lengthscale of the scalar field the faster the mixing (and hence the scalar variance decay). This effect can be captured only if the mixing model contains some representation of the length scales associated with the scalar field.

### Flamelet Combustion

In flamelet combustion the scalar gradients (of the reactive scalars) are enhanced by reaction. As a consequence the assumption that the diagonal elements of the "joint" dissipation tensor are determined solely by the large scales of the turbulence is no longer valid. Extension of current mixing models to the flamelet limit requires incorporating the effect of steepening of scalar gradients due to reaction.

### Examples of Pairwise Exchange Models

It is convenient to view the locations of the nonzero entries in the interaction matrix as representing "edges" connecting particles in composition space, along which particles interact in a model of the mixing process. The values of these nonzero entries can be thought of as coefficients associated with these edges, which control the rate at which the two particles at either end of the edge are attracted to each other (note that for a symmetric interaction matrix the off-diagonal entries must all be negative). Different choices of edges, and different values of their coefficients result in different mixing models.

Models like Curl's model [15] and its variants, IEM [4], and the mapping closure particle

model for a single scalar are all pairwise exchange models (or can be expressed as such). In Curl's model mixing is achieved by subjecting the ensemble to the following stochastic process over a sequence of small time steps  $\Delta t$  ( $\Delta t \langle \omega \rangle \ll 1$ , where  $\langle \omega \rangle = \epsilon/k$  is the mean turbulent frequency in the cell,  $k$  and  $\epsilon$  being the turbulent kinetic energy and its dissipation rate respectively). Particle pairs are selected at random from the ensemble, with  $N_p$  pairs selected ( $N_p$  is the minimum number of particle pairs such that the sum of the weights of selected particles exceeds  $\Delta t \langle \omega \rangle$ ). If the two members in the pair are denoted  $n$  and  $m$ , mixing is performed by changing the compositions to

$$\phi_{\beta n}(t + \Delta t) = \phi_{\beta}^*, \quad (25)$$

$$\phi_{\beta m}(t + \Delta t) = \phi_{\beta}^*,$$

where,

$$\phi_{\beta}^* = \frac{w_{(n)}\phi_{\beta n} + w_{(m)}\phi_{\beta m}}{w_{(n)} + w_{(m)}}. \quad (26)$$

This mixing process is performed for each of the  $N_p$  pairs selected to produce the ensemble at time  $t + \Delta t$ . For particles not selected, their compositions are unaltered. While in Curl's model particle composition values change discontinuously in time (whereas Eq. 11 represents a continuous change of composition), Curl's model can still be represented by a discrete time version of Eq. 11, namely

$$\Delta \phi_{\beta i} = -\frac{1}{w_{(i)}} \sum_{j=1}^N M_{ij} \phi_{\beta j} \Delta t,$$

with interaction matrix  $\mathbf{M}$  such that the  $m^{th}$  row corresponding to that member in the particle pair has entries:

$$M_{(m)(m)} = \frac{w_{(m)}w_{(n)}}{w_{(n)} + w_{(m)}}$$

$$M_{mn} = -\frac{w_{(m)}w_{(n)}}{w_{(n)} + w_{(m)}}$$

$$M_{mk} = 0, \quad k \neq m, \quad k \neq n.$$

The apparent discrepancy in the dimension of  $\mathbf{M}$  arises from the fact that the fraction of particle pairs selected results in an inverse time term in the pdf evolution equation [16]. Curl's model satisfies the conservation of means and

decay of variance criteria by virtue of being a pairwise-exchange model. It also satisfies boundedness and independence principles. However, it does not satisfy the localness principle since the particle pair selected for mixing may be drawn from anywhere in composition space. As noted previously [16], since the composition changes discontinuously in Curl's model, it is incapable of generating a differentiable scalar cumulative distribution function (cdf) from an initially nondifferentiable cdf.

For the IEM model [4], the  $i^{th}$  particle's compositions evolve as

$$\frac{d\phi_{\beta i}}{dt} = -\frac{1}{2} C_{\phi} \langle \omega \rangle (\phi_{\beta i} - \langle \phi_{\beta} \rangle), \quad (27)$$

where  $C_{\phi}$  is a model constant chosen to be 2.0 to yield the desired scalar variance decay rate. Since  $\langle \phi_{\beta} \rangle$  is usually estimated by simple averaging of the particle compositions within a cell, the IEM model can also be cast in the interaction matrix form with  $\mathbf{M}$  now given by,

$$M_{(i)(i)} = \frac{1}{2} C_{\phi} \langle \omega \rangle (1 - w_{(i)})w_{(i)}$$

$$M_{ij} = -\frac{1}{2} C_{\phi} \langle \omega \rangle w_{(j)}w_{(i)}, \quad i \neq j.$$

The IEM model also satisfies the conservation of means and variance decay criteria by virtue of being a pairwise-exchange model. It also satisfies the boundedness and independence principles. However, it does not satisfy the localness principle since the particle composition mixes toward the mean composition value:  $M_{ij}$  is nonzero for all  $i$  and  $j$ .

Even the computational stencil for direct numerical simulations can be cast in the particle interaction form. Mixing models such as the binomial Langevin mixing model [17] and the Fokker-Planck closure model [18] are examples of models that are not members of this class. The mixing model to be described in this paper also belongs to the class of particle interaction mixing models.

### Implications for the EMST Model

It is a formidable task to construct a mixing model which performs well with respect to all of the above performance criteria. Moreover some of these criteria (scalar length scale depen-

dence, flamelet combustion) cannot be directly addressed at the current level of closure (namely, one-point, one-time Eulerian pdf of scalar amplitude). However, attempting a higher level of closure raises several issues such as: (i) consistent extension of the velocity model to this level of closure, (ii) difficulties in modeling due to lack of information (either from experiments or DNS) about the unclosed terms at the new level of closure, (iii) computational expense and numerical issues. In this paper, an attempt is made to satisfy selectively those criteria which we believe are most important in reactive flow applications; namely localness and boundedness, at the one-point, one-time scalar amplitude level of closure, in a computationally tractable model.

Since the EMST mixing model is an extension of the form of the mapping closure particle equations to multiple scalars using the Euclidean minimum spanning tree in composition space, it is advantageous to first consider the 1-D mapping closure model.

## MAPPING CLOSURES

Mapping closures for turbulent mixing were proposed by Chen et al. [19] and a particle implementation of this model for a single scalar was described by Pope [20]. The salient aspects of this model which are pertinent to the EMST mixing model are briefly reviewed here.

In the mapping closure formalism, a statistically homogeneous, isotropic, time-independent Gaussian random field (with standardized normal cumulative distribution function (cdf)  $G(\eta)$ ) is mapped through a mapping  $X(\eta, t)$  to a statistically homogeneous scalar field (with cdf  $F(\psi; t)$ ) evolving in a turbulent flow, such that

$$F(X(\eta, t); t) = G(\eta). \quad (28)$$

While the evolution equation of the scalar cdf (or pdf) contains unclosed terms, these can be expressed in terms of the known statistics of the Gaussian reference field and properties of the mapping. This model has been applied to the case of a single inert, passive, statistically homogeneous scalar field evolving in isotropic turbulence and the analytic model solution [20] for this problem shows remarkably close agreement with the direct numerical simulations of Eswaran and Pope [12]. The mapping closure for a

single scalar yields a mixing model that is local in composition space (as is shown later in this section) and also satisfies the performance criteria of mean conservation, variance decay, boundedness, and relaxation to a Gaussian. However, there are difficulties in extending mapping closures to multiple reactive scalars since the mappings are nonunique and expensive to compute. Hence, an alternative approach to generalizing the mapping closure mixing model to multiple scalars is considered via its particle implementation with the aim of retaining as many of its desirable properties listed above.

In a particle method solution of the pdf transport equation, the pdf  $f(\psi; t)$  at time  $t$  of a homogeneous scalar field  $\phi(\mathbf{x}, t)$  ( $\psi$  being the sample space variable of  $\phi$ ) is indirectly represented by an ensemble of  $N$  particles with composition  $\phi_i$  and weight  $w_{(i)}$ ,  $i = 1, \dots, N$ . Since the condition for uniqueness of the mapping requires that it be a nondecreasing function of its argument, this requires that the particles are first sorted in nondecreasing order of composition value such that

$$\phi_1 \leq \phi_2 \leq \dots \leq \phi_N.$$

The discrete representation of the mapping equation (Eq. 28) is expressed by the correspondence between the points  $\eta_{i+1/2}$  (in the sample space of the Gaussian reference field) and  $\psi_{i+1/2}$  (in the sample space of the scalar) through the cdf's  $F$  and  $G$ :

$$\begin{aligned} F(\psi_{i+1/2}; t) &= F(X(\eta_{i+1/2}, t); t) \\ &= G(\eta_{i+1/2}) \\ &= \sum_{j=1}^i w_{(j)}, \end{aligned} \quad (29)$$

see Fig. 2. From the mapping evolution equation [20], the evolution of each particle's composition can be derived with the only approximation being a finite-difference approximation for the mapping gradient in sample space. The evolution equation for the particle composition is

$$\begin{aligned} w_{(i)} \frac{d\phi_{(i)}}{dt} &= \frac{1}{\tau_{MC}} [-B_{i+1/2}(\phi_i - \phi_{i+1}) \\ &\quad - B_{i-1/2}(\phi_i - \phi_{i-1})], \end{aligned} \quad (30)$$

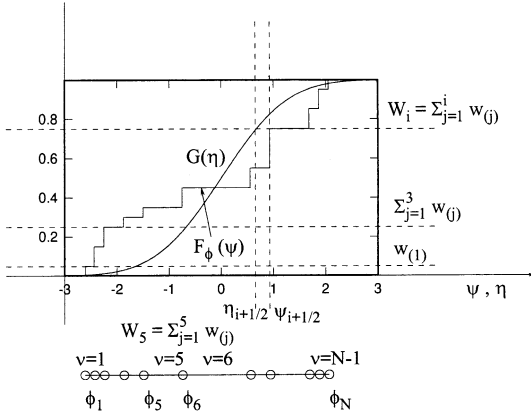


Fig. 2. Cumulative distribution function  $F_\phi(\psi)$  (discrete representation) of a single scalar  $\phi$  and mapping of  $\psi_{i+1/2}$  to  $\eta_{i+1/2}$  through the Gaussian cdf  $G(\eta)$ . Also shown are the 1-D edge list and the particle and cumulative edge weights.

where  $B_{i\pm 1/2}$  are model coefficients given by

$$B_{i+1/2} \equiv \frac{g(\eta_{i+1/2})}{[\eta_{i+1} - \eta_i]}, \quad i = 1, \dots, N - 1. \tag{31}$$

In Eq. 31  $g(\eta)$  represents the standardized normal density function and  $\eta_i = (\eta_{i-1/2} + \eta_{i+1/2})/2$ . The factor  $\tau_{MC}$  in Eq. 30 is the characteristic time associated with the mapping closure model and is a function of the scalar diffusivity, and properties of the mapping and reference field [20].

The mapping closure particle model is also a pairwise-exchange model and hence satisfies mean conservation and variance decay. It also satisfies the boundedness principle. Each particle evolves by interaction with its neighbor particles (in composition space) and the rate of attraction is given by  $B_{i\pm 1/2}$  (with  $B_{1/2} = 0$ ,  $B_{N+1/2} = 0$ ). Clearly, this model also satisfies the localness principle.

The mapping closure model can be expressed as a particle exchange model with interaction matrix coefficients:

$$\begin{aligned} M_{(i)(i)} &= (B_{i+1/2} + B_{i-1/2})/\tau_{MC} \\ M_{(i)(i+1)} &= -B_{i+1/2}/\tau_{MC} \\ M_{(i)(i-1)} &= -B_{i-1/2}/\tau_{MC}, \quad i = 1, \dots, N. \end{aligned}$$

Extension of this model to higher scalar dimensions requires (a) a definition of localness

that is valid in any dimension, and (b) generalization of the form of the particle composition evolution equation (Eq. 30). Definitions of localness will be discussed in subsequent sections, but the issue of generalizing Eq. 30 is considered here.

For the case of a single scalar each particle evolves by interaction with its two adjacent neighbors (except for the extremum scalar values which have only one neighbor each). For two or more scalars there is no reason to restrict the number of neighbors to two and the evolution equation needs to be modified to reflect this. Further the specification of the interaction coefficients needs to be generalized for any number of scalar dimensions.

With this generalization in mind it is convenient to associate the interaction coefficients  $B_{i\pm 1/2}$  with the particle pairs whose evolution they affect. Denoting the unordered particle pair  $(m_\nu, n_\nu)$  to be the  $\nu^{th}$  edge, the coefficient associated with this edge is denoted  $B_\nu$ . Now the evolution equation for the particle composition can be rewritten as

$$\begin{aligned} w_{(i)} \frac{d\phi_{(i)}}{dt} &= -\tau_{MC}^{-1} \sum_\nu B_\nu \{ (\phi_{(i)} - \phi_{n_\nu}) \delta_{im_\nu} \\ &\quad + (\phi_{(i)} - \phi_{m_\nu}) \delta_{in_\nu} \}, \end{aligned} \tag{32}$$

where the  $\nu^{th}$  edge connects the particle pair  $(m_\nu, n_\nu)$  and  $\delta$  represents the Kronecker delta. Summing over the list of edges, the term in braces is nonzero when the particles  $m_\nu$  and  $n_\nu$  are connected by the  $\nu^{th}$  edge. Since the edge is an unordered particle pair, either combination needs to be accounted for by the two terms with Kronecker  $\delta$ 's. This model is also a pairwise exchange model since the same coefficient  $B_\nu$  appears in the evolution equation of  $m_\nu$  as well as in  $n_\nu$ .

Of course for the 1-D mapping closure each particle with index  $1 < i < N$ , has exactly two edges incident on it. The extremum particles  $i = 1$  and  $i = N$  have only one edge incident on them. Given the list of particle indices ordered by composition value, an edge list is trivially generated by defining the  $\nu^{th}$  edge as connecting particles  $\nu$  and  $\nu + 1$ , for  $1 \leq \nu \leq N - 1$ . See Fig. 2.

For the single scalar case there exists a one-

to-one relationship between an edge in the edge list defined by this procedure and the location of the corresponding particle pair connected by the edge in composition space. This relationship is established by associating a cumulative edge-weight with each edge. For the  $\nu^{th}$  edge this can be defined as

$$W_\nu = \sum_{i=1}^{\nu} w_{(i)}. \tag{33}$$

The cumulative edge-weight is a minimum at the minimum scalar value of the distribution and increases monotonically until we approach the maximum scalar value where it takes the maximum value of 1. As an example (assuming even  $N$  and equal particle weights  $w_{(i)} = 1/N$ ), the first edge (with cumulative edge-weight  $1/N$ ), connects  $\phi_1$  to  $\phi_2$ , and the edge with index  $N/2$  (cumulative edge weight  $1/2$ ) connects particles with index  $N/2$  and  $N/2 + 1$  which lie near the median of the distribution.

For the 1-D mapping closure the coefficients  $B_\nu$  are solely a function of the cumulative edge-weight. In the limit of  $N \rightarrow \infty$  this function has an analytic form (expressible in terms of the standardized Gaussian density) and is symmetric with respect to the cumulative edge-weight ( $W_\nu$ ) value of  $1/2$  [20].

Exploiting this symmetry, a quantity called the edge-weight  $w_\nu$  can be associated with the  $\nu^{th}$  edge such that

$$w_\nu = \min(W_\nu, \bar{W}_\nu) \tag{34}$$

where  $\bar{W}_\nu = \sum_{i=\nu+1}^N w_{(i)}$ .

The edge-weight defined in this way is a minimum at the extremal values of the distribution and increases as we approach the median where it takes the maximum value of  $1/2$ . Note that edges corresponding to different particle pairs can have the same edge-weight. For the single scalar case exactly two such edges will have the same edge-weight. In higher dimensions more than two edges can have the same edge-weight.

Since the coefficients  $B_\nu$  are symmetric with respect to the cumulative edge-weight ( $W_\nu$ ), they can be expressed as a function of only the edge-weight  $w_\nu$ . See Fig. 3. This functional

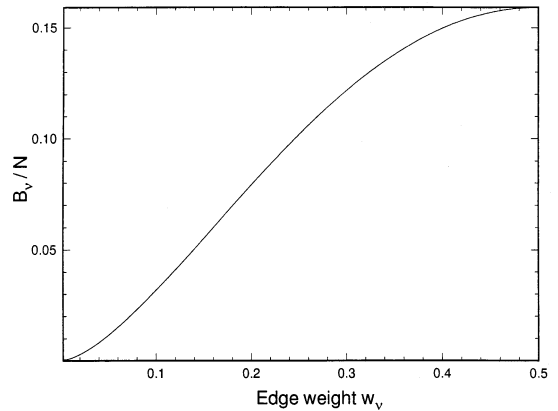


Fig. 3. Coefficient  $B_\nu/N$  vs. edge-weight  $w_\nu$  for the 1-D mapping closure.

dependence is generalized in the EMST model which is described in the following section.

### EMST MIXING MODEL

In modeling the mixing of a single scalar, where the composition space is one-dimensional, a simple ordering of the particle scalar values provides *the* definition of localness. For this case the mapping closure particle model provides an adequate description of the evolution of a particle’s composition by interaction with its neighbor particles in composition space. In modeling the mixing of multiple scalars, where the composition space is of a dimension higher than one, a particle interaction mixing model that is local requires a definition of neighboring particles. The Euclidean minimum spanning tree (described in the following subsection) constructed on the ensemble of particles in composition space of arbitrary dimension provides one such definition of neighbor particles. A particle’s composition then evolves as per the generalized version of the mapping closure evolution equation (Eq. 32).

However, results obtained using this model for the problem of two statistically identical initially joint-normal scalars evolving under the influence of imposed linear mean scalar gradients in isotropic turbulence (described in the next section) show that the model produces unphysical scalar joint pdf’s which are no longer joint-normal. In this problem the fluctuating scalar fields are homogeneous. In the simulation

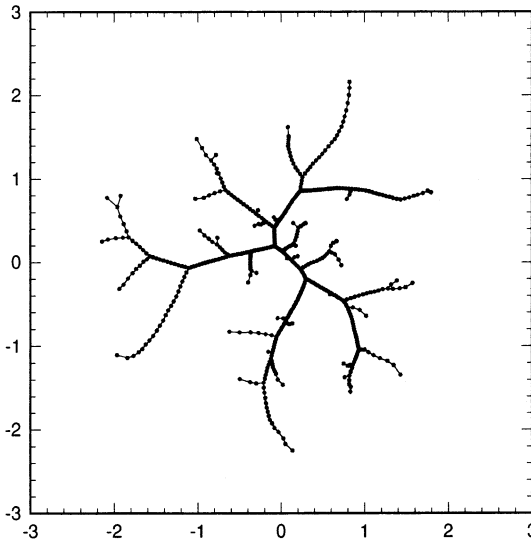


Fig. 4. An example of “stranding”: scatter plot of particles in 2-D composition space with EMST superimposed at  $t = 0.5\tau_\phi$  in the mean scalar gradient test using EMST mixing without intermittency; initial distribution was joint-normal.

particle properties evolve from the specified initial conditions but since no new particles enter (or leave) the domain, the ensemble of particles remains unchanged. As a consequence the EMST in the 2-D composition space is formed on the same ensemble of particles. This results in repeated attraction of any given particle to the same restricted set of neighbor particles (which is not consistent with the physical process of mixing where a fluid particle’s composition changes as a result of interaction with the entire composition field in its neighborhood), and hence the ensemble of particles collapses along “strands” in composition space (see Fig. 4).

In order to alleviate this “stranding” problem, an intermittency feature is introduced into the EMST mixing model. At any given time a particle is in one of two states: a mixing state where its composition changes due to mixing, or a nonmixing state where its composition is unchanged due to mixing. A nondimensional age property is associated with each particle which determines how long a particle mixes and how long it is in the nonmixing state. The time a particle spends in both the mixing and nonmixing states is bounded. With the addition of this feature the EMST is now formed based only on those particles that are in the mixing state at that instant of time. Results obtained for the

EMST mixing model using this feature are satisfactory and are described in the next section.

The following subsections are devoted to describing the EMST mixing model with the intermittency feature. This is followed by a description of model parameters and coefficients. The section concludes with a discussion of the various model features and its properties.

### EMST Model Implementation

Consider an inhomogeneous flow where the solution domain in physical space is discretized into a number of cells. To a first approximation the property fields in a cell can be assumed to be statistically homogeneous and the joint pdf of compositions is represented by an ensemble of  $N$  particles  $\phi_{\beta i}$ ,  $\beta = 1, \dots, D$ ,  $i = 1, \dots, N$ , where  $D$  is the dimension of the composition space. In some of the illustrations that follow, we consider two scalars ( $D = 2$ ). An ensemble of particles drawn from the specified initial composition jpdf (in this case chosen to be an uncorrelated joint-normal) can be represented as a scatter plot in composition space as shown by the circles (open and filled) in Fig. 5.

At any given time only a subset (referred to as the mixing subset) of the total ensemble of  $N$  particles participates in the mixing process. Whether or not a particle belongs to the mixing subset is determined by a nondimensional particle age property,  $Z^{(i)}$ , associated with each particle. The initialization and evolution of this age property is now described.

### Intermittency

If the particle age property is positive  $Z^{(i)} > 0$  (referred to as state 1), the particle is in the mixing subset, otherwise if  $Z^{(i)} \leq 0$  (referred to as state 0), then the particle is not in the mixing subset. The time a particle spends in the mixing and nonmixing states is required to scale with the timescale of turbulence in the cell. If  $k$  is the turbulent kinetic energy and  $\epsilon$  is the mean dissipation rate, then  $\langle \omega \rangle = \epsilon/k$  represents the mean turbulent frequency (the reciprocal of the turbulence timescale). A scaled time can now be defined in terms of the mean turbulent frequency ( $\langle \omega \rangle$ ) and the physical time  $t$  by

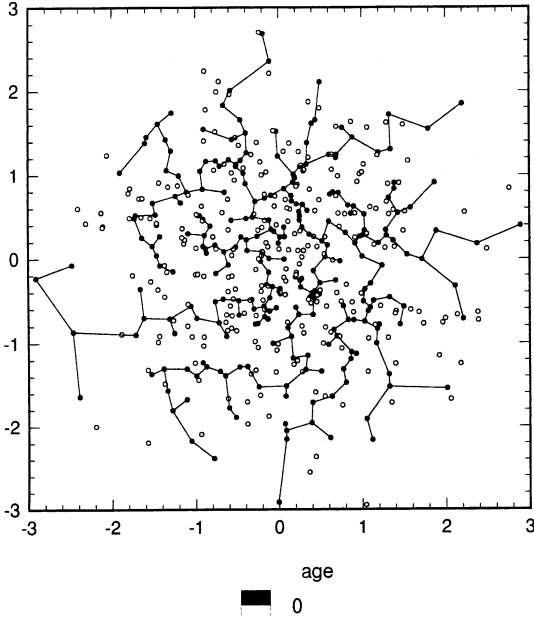


Fig. 5. Euclidean minimum spanning tree constructed on the mixing subset of an ensemble of particles in 2-D composition space (open circles represent particles in the nonmixing state with  $Z < 0$ );  $N = 512$  particles, joint-normal distribution.

$$s \equiv s_0 + \int_0^t \langle \omega \rangle(t) dt,$$

where  $s_0$  is the origin of the scaled time which can be fixed arbitrarily.

Each particle's age property  $Z^{(i)}$  is chosen to be a realization of a stochastic process  $Z(s)$  (called the age process), which evolves in  $s$ , the scaled time. Figure 6 shows a sketch of the age process  $Z(s)$ . When the particle age is positive it decreases linearly until it reaches zero where it discontinuously jumps to a negative value. At any instant a positive particle age represents the

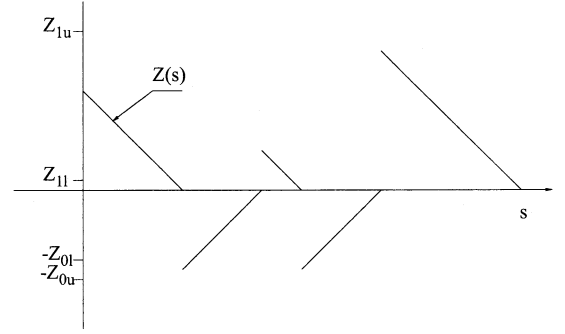


Fig. 6. The age process  $Z(s)$  versus scaled time  $s$ .

excess life (in scaled time) the particle has to participate in the mixing process. A negative particle age represents the waiting time before the particle mixes again.

The evolution of the age process can be written as follows. For infinitesimal positive  $ds$ ,

$$Z(s + ds) = Z(s) - ds, \text{ for } Z(s) > ds \quad (35)$$

$$Z(s + ds) = Z(s) + ds, \text{ for } Z(s) < -ds$$

$$Z(s + ds) \stackrel{D}{=} \mathcal{U}_1(z), 0 \leq Z(s) \leq ds$$

$$Z(s + ds) \stackrel{D}{=} \mathcal{U}_0(z), -ds \leq Z(s) \leq 0$$

where  $\mathcal{U}_1(z)$  and  $\mathcal{U}_0(z)$  are uniform random variables in the intervals  $[Z_{1l}, Z_{1u}]$ , and  $[Z_{0l}, Z_{0u}]$  respectively.

For stationary homogeneous turbulence the mean turbulent frequency is constant and the scaled time is linearly related to the physical time. For this case we require the age process to admit a stationary solution. It can be shown from the theory of renewal processes [21] that this is achieved if the initial age distribution,  $G(z)$ , is specified as follows:

$$\begin{aligned} G(z) &= (1 - p_0) + p_0 \left\{ \frac{2z}{Z_{1l} + Z_{1u}} \right\}, 0 < z \leq Z_{1l} \\ &= (1 - p_0) + p_0 \left\{ \frac{2Z_{1l}}{Z_{1l} + Z_{1u}} + \frac{[2Z_{1u}(z - Z_{1l}) - (z^2 - Z_{1l}^2)]}{Z_{1u}^2 - Z_{1l}^2} \right\}, Z_{1l} < z \leq Z_{1u} \\ &= (1 - p_0) \left\{ 1 - \frac{2|z|}{Z_{0l} + Z_{0u}} \right\}, -Z_{0l} < z \leq 0 \\ &= (1 - p_0) \left\{ 1 - \frac{2Z_{0l}}{Z_{0l} + Z_{0u}} - \frac{[2Z_{0u}(|z| - Z_{0l}) - (z^2 - Z_{0l}^2)]}{Z_{0u}^2 - Z_{0l}^2} \right\}, -Z_{0u} < z \leq -Z_{0l} \end{aligned}$$

where  $p_0$  is the fraction of the total ensemble of particles which is initially assigned to the mixing state ( $Z(0) > 0$ ). In other words

$$P[Z(0) > 0] = 1 - G(0) = p_0. \quad (36)$$

If  $I(s)$  is the indicator function for the process  $Z(s)$  being positive (i.e., the particle is in a mixing state), then it can be shown that for stationary homogeneous turbulence

$$\lim_{s \rightarrow \infty} \frac{1}{s} \int_0^s I(u) du = \frac{\langle Z_1 \rangle}{\langle Z_0 \rangle + \langle Z_1 \rangle}, \quad (37)$$

where the absolute value of the positive and negative jumps in  $Z(s)$  each time the process hits zero are represented by the random variables  $Z_1$  and  $Z_0$  respectively. In other words Eq. 37 states that time a particle spends on average in the mixing state is given by the ratio of the average positive jump to the sum of the average positive and negative jumps taken by the age process  $Z(s)$ . The specified initial distribution will be a stationary solution to the age process evolution equation only if  $p_0$  is chosen such that

$$p_0 = \frac{\langle Z_1 \rangle}{\langle Z_0 \rangle + \langle Z_1 \rangle}. \quad (38)$$

For the general inhomogeneous problem  $\langle \omega \rangle$  varies from cell to cell and could also be a function of time. However, since the age process is defined in terms of nondimensional quantities its initialization and evolution remain unchanged.

If there are  $N$  particles in a cell at any given time  $t$ , the  $N_T$  particles that make up the subset of this ensemble that participate in the mixing process is determined based on the age-property of each particle:

$$N_T(t) = \sum_{i=1}^N H(Z^{(i)}(s)), \quad (39)$$

where  $H(z)$  is the Heaviside function.

### Definition of the EMST

Loosely speaking, constructing the EMST on the mixing subset of  $N_T$  particles requires connecting every particle with at least one neighbor particle through an edge (an unordered pair of

particles). Since every particle is connected in the EMST it possesses the spanning property. A tree is a set of edges that contains no closed loops or cycles; i.e., starting from a particle, tracing an alternating sequence of edges and particles terminating in a particle, does not lead back to the initial particle. Finally since it is a Euclidean minimum spanning tree, the sum of the Euclidean lengths of these edges is a minimum. A formal graph-theoretic definition of a minimum spanning tree (MST) and algorithms for constructing an MST can be found in the literature [22], [23].

The EMST in composition space constructed on the mixing subset of the ensemble of particles representing two scalars joint-normally distributed is shown in Fig. 5. It can be shown that a tree constructed on  $N_T$  particles has  $N_T - 1$  edges [24]. The EMST on  $N_T$  particles is thus defined by the set of  $N_T$  particles and the  $N_T - 1$  edges that connect them.

The temporal behavior of the EMST constructed on the mixing subset of particles in a particular computational cell in an inhomogeneous flow can be qualitatively described as follows: Particles enter and leave the cell as they move through physical space according to their particle velocity. Depending on their age property they are divided into mixing and nonmixing subensembles and the EMST is formed on the mixing subset. Consequently, in the general inhomogeneous case, the EMST changes discontinuously in time due to particles that are in the mixing state entering/leaving the cell, and due to particles in the cell entering/leaving the mixing state.

### Particle Composition Evolution

Each edge in the EMST is assigned an edge-weight which is defined analogously to the edge-weight definition in the mapping closure particle implementation. Let  $\nu$  denote the edge that connects particles  $m_\nu$  and  $n_\nu$ . If this edge were removed from the set of EMST edges, then the remaining set of edges define two subtrees one of which (denoted  $T_{m_\nu}$ ) contains particle  $m_\nu$ , and the other (denoted  $T_{n_\nu}$ ), particle  $n_\nu$ . Each of these subtrees consists of a set of edges and the particles that are connected by these edges. Each of these subtrees  $T_{m_\nu}$  and  $T_{n_\nu}$  is assigned a

weight ( $W_{T_{m_\nu}}$  and  $W_{T_{n_\nu}}$  respectively) which is defined as the sum of the weights of the particles that belong to that subtree. Mathematically,

$$W_{T_{m_\nu}} = \sum_{k \in T_{m_\nu}} w(k)$$

$$W_{T_{n_\nu}} = \sum_{k \in T_{n_\nu}} w(k).$$

The edge-weight of edge  $\nu$  is now defined as

$$w_\nu = \min(W_{T_{m_\nu}}, W_{T_{n_\nu}}). \quad (40)$$

Since the particle weights sum to unity, the edge-weight ranges from the minimum particle weight to 1/2.

An edge coefficient  $B_\nu$  is associated with the  $\nu^{\text{th}}$  edge analogous to the mapping closure particle model. The edge-coefficient is chosen to be a linear function of the edge-weight:

$$B_\nu = 2w_\nu.$$

The choice of this edge-coefficient is discussed later in this section. Since the edge-weight is maximized by 1/2, the edge-coefficient is bounded by unity.

As in the mapping closure particle model, a particle's composition evolves by interaction with its neighbors in composition space. The neighbors of a particle are defined by the edges in the EMST that are incident on the particle. Using these definitions the evolution equation for the vector of particle compositions  $\phi_{(i)} = \phi_{\beta(i)}$ ,  $\beta = 1, \dots, D$ ,  $i = 1, \dots, N_T$  can be written as (cf. Eq. 32)

$$w_{(i)} \frac{d\phi_{(i)}}{dt} = -\alpha \sum_{\nu=1}^{N_T-1} B_\nu \{ (\phi_{(i)} - \phi_{n_\nu}) \delta_{im_\nu} + (\phi_{(i)} - \phi_{m_\nu}) \delta_{in_\nu} \}, \quad (41)$$

where the  $\nu^{\text{th}}$  edge connects the particle pair  $(m_\nu, n_\nu)$  and  $\delta$  represents the Kronecker delta. This model is also a pairwise exchange model since the same coefficient  $B_\nu$  appears in the evolution equation of  $m_\nu$  as well as  $n_\nu$ , and this coefficient is a function solely of the edge-weight (which by definition is the same for either particle belonging to the edge). The parameter  $\alpha$  is determined by requiring that the scalar variances decay at a prescribed rate and it is described later in this section.

The matrix form of EMST model evolution (Eq. 41) is

$$\frac{d\phi_{\beta i}}{dt} = -\frac{1}{w_{(i)}} M_{ij} \phi_{\beta j}, \quad i = 1, \dots, N_T, \quad (42)$$

with the interaction matrix elements given by

$$M_{ij} = -\alpha \sum_{\nu=1}^{N_T-1} B_\nu \{ \delta_{im_\nu} \delta_{jn_\nu} + \delta_{jm_\nu} \delta_{in_\nu} \}, \quad j \neq i$$

$$M_{(i)(i)} = \alpha \sum_{j=1}^{N_T} \sum_{\nu=1}^{N_T-1} B_\nu \{ \delta_{im_\nu} \delta_{jn_\nu} + \delta_{jm_\nu} \delta_{in_\nu} \}.$$

It is convenient at this point to also define

$$\bar{M}_{ij} \equiv \frac{1}{\alpha} M_{ij}.$$

### Model Parameters

In this subsection the choice of model parameters and coefficients is described and model sensitivity to variation of these parameters is discussed qualitatively.

### Model Coefficients

The choice of  $B$  coefficients is crucial in determining the evolution of the composition jpdf. These edge coefficients are assumed to be a function of only the edge-weight in the spirit of the mapping closure model. Their choice is determined by the criterion that in the mean scalar gradient test problem, an initially joint-normal composition jpdf (dimension of composition space  $D = 2$ ) remains joint-normal. After numerical experimentation with several different functions of edge-weight, a linear function  $B_\nu = 2w_\nu$  was chosen to be the model specification. This specification resulted in an evolution to composition jpdf's that are close to (but not exactly) joint-normal for the mean scalar gradient test case with two scalars. Comparable results were also obtained for five and 10 scalars.

The following general observations can be made about the  $B$  coefficients. Since particles that lie at the extrema of the distribution are more likely to have only one edge incident on them (such particles are called leaves), they correspond to the lowest edge-weight. (Note that the converse is not true). Hence, a relative increase in the  $B$  coefficient values at lower

edge-weights will cause the tails of the composition jpdf to be drawn in faster.

For a given distribution of scalars, the distribution of edge-weight changes as the dimensionality of the scalar space ( $D$ ) is increased. In an effort to keep the model as simple as possible, there is no dependence of the  $B$  coefficients on  $D$ . As the dimensionality of the composition space increases, the probability of finding leaves increases and it is reasonable that the  $B$  coefficient values at the lowest and highest edge-weight predominantly govern the model evolution. Consequently, as the number of compositions increases the model is expected to show decreased sensitivity to the choice of  $B$  in the intermediate range of edge-weights.

### Determination of $\alpha$

The model parameter  $\alpha$  controls the rate of variance decay of the scalars, and its specification is described in this subsection.

Consider a single conserved passive scalar field with mean  $\langle\phi\rangle$  and variance  $\langle\phi'^2\rangle$  evolving in constant-density homogeneous turbulence. The mean is unaffected by the mixing, hence

$$\frac{d\langle\phi\rangle}{dt} = 0.$$

The scalar variance evolution can be written as

$$\frac{d\langle\phi'^2\rangle}{dt} = -\frac{\langle\phi'^2\rangle}{\tau_\phi},$$

such that the scalar variance decays exponentially with a scalar timescale  $\tau_\phi$ . Following standard modeling assumptions [1],  $\tau_\phi$  can be related to the timescale of the turbulence ( $\tau \equiv k/\epsilon$ ) by

$$\tau_\phi = \tau/C_\phi,$$

where the empirical constant  $C_\phi$  is taken to be 2.0. The parameter  $\alpha$  is chosen such that the ensemble variance evolution implied by the EMST model evolution equation obeys the same decay law. This is accomplished by first expressing the variance decay rate implied by the EMST model equation in terms of  $\alpha$  and a function of the ensemble composition values. This EMST model variance decay rate is then equated to the desired variance decay rate and the value of  $\alpha$  that satisfies this equality is solved for.

The ensemble scalar variance evolution is given by

$$\begin{aligned} \frac{d\langle\phi'^2\rangle_N}{dt} &= \sum_{i=1}^{N_T} w_{(i)} 2\phi'_{(i)} \frac{d\phi'_{(i)}}{dt} \\ &= -\alpha \sum_{i=1}^{N_T} w_{(i)} 2\phi'_{(i)} \bar{M}_{ij} \phi'_j. \end{aligned} \quad (43)$$

Equating this to the desired decay rate and solving for  $\alpha$  yields

$$\alpha = \frac{\langle\phi'^2\rangle_N}{\tau_\phi \sum_{i=1}^{N_T} w_{(i)} 2\phi'_{(i)} \bar{M}_{ij} \phi'_j}. \quad (44)$$

For multiple scalars the choice of  $\alpha$  is not as straightforward. In general this parameter is to be chosen such that it yields a prescribed behavior for some function of the covariance matrix which is called the variance function. Since each scalar does not evolve independently in the EMST model, requiring that one of the scalars obey a specific decay law imposes a decay law on the other scalars (which may not be consistent with standard modeling). One way to circumvent this problem is to require that  $\alpha$  be based on the trace of the covariance matrix. The variance function is defined to be the trace of the covariance matrix

$$\Sigma = C_{\beta\beta}.$$

If each scalar decays with the same scalar timescale  $\tau_\phi$ , then the variance function obeys the evolution equation

$$\frac{d\Sigma}{dt} = -\frac{\Sigma}{\tau_\phi} = -\frac{C_\phi \Sigma}{\tau}. \quad (45)$$

The EMST model evolution in matrix form for multiple scalars is

$$w_{(i)} \frac{d\phi_{\beta(i)}}{dt} = -\alpha \sum_{j=1}^{N_T} \bar{M}_{ij} \phi_{\beta j}, \quad i = 1, \dots, N_T, \quad (46)$$

Similar to the single scalar case, the variance function evolution can be written as

$$\begin{aligned} \frac{d\Sigma}{dt} &= \sum_{i=1}^{N_T} w_{(i)} 2\phi'_{\beta(i)} \frac{d\phi'_{\beta(i)}}{dt} \\ &= -\alpha \sum_{i=1}^{N_T} w_{(i)} 2\phi'_{\beta(i)} \bar{M}_{ij} \phi'_{\beta j}. \end{aligned}$$

Equating this to the desired decay rate and solving for  $\alpha$  yields

$$\alpha = \frac{\Sigma}{\tau_\phi \sum_{i=1}^{N_T} w_{(i)} 2\phi'_{\beta(i)} \bar{M}_{ij} \phi'_{\beta j}}. \quad (47)$$

Though the expression for  $\alpha$  in continuous time is written explicitly in terms of known quantities, in practice the value of  $\alpha$  has to be determined at each time step in the Monte Carlo simulation such that the variance function satisfies the prescribed decay law. Since the variance function is a nonlinear function of time, a root finding technique is needed to compute the parameter  $\alpha$ . The root finder typically converges in 2 or 3 iterations.

### Age Process Parameters

In the age process specification there are five model parameters, namely  $p_0$ ,  $Z_{1_t}$ ,  $Z_{1_u}$ ,  $Z_{0_t}$ , and  $Z_{0_u}$ . In view of Eq. 38, only four of these parameters are independent. In the model these four parameters are specified indirectly by specifying  $p_0$ ,  $\langle Z_0 \rangle$ ,  $Z_{w_0}$ , and  $Z_{w_1}$ , where

$$Z_{0_t} = \langle Z_0 \rangle - Z_{w_0}$$

$$Z_{0_u} = \langle Z_0 \rangle + Z_{w_0}$$

$$Z_{1_t} = \langle Z_1 \rangle - Z_{w_1}$$

$$Z_{1_u} = \langle Z_1 \rangle + Z_{w_1}.$$

The specification of each of these parameters is now considered. As  $p_0$  approaches unity the effect of intermittency decreases until there is no intermittency at  $p_0 = 1$ . As  $p_0$  approaches zero the effect of intermittency increases, but  $p_0$  cannot be decreased arbitrarily in view of Eq. 47. As the number of particles that participate in the mixing process at initial time  $N_T(0)$  (and at all times for the homogeneous test cases where the age process is stationary) decreases, their compositions need to decay at faster rates in order to yield the same decay rate for the variance function based on the total ensemble of particles. In practice the maximum decay rate of the composition of mixing particles is limited by a threshold value which is a multiple (chosen to be 2.5) of the mixing frequency  $\langle \omega_\phi \rangle$ , where  $\langle \omega_\phi \rangle = 1/\tau_\phi = C_\phi \langle \omega \rangle$ . If the variance function decay timescale is specified by  $\tau_\phi = \tau/C_\phi$ , then given a maximum decay rate threshold, there

exists a minimum  $p_0$  above which a solution to Eq. 47 exists. In the limit of  $N \rightarrow \infty$  and for the values considered ( $C_\phi = 2.0$  and maximum decay rate =  $2.5 \times \langle \omega_\phi \rangle$ ) this gives  $p_{0_{\min}} = 1/2.5 = 0.4$ . The fraction of the total ensemble of particles which is initially assigned to the mixing state  $p_0$  is chosen to be  $1/2$ .

The parameter  $\langle Z_0 \rangle$  determines the average time that a particle spends in the nonmixing state after it changes from a mixing state. This is chosen to be  $1/6$  based on numerical experiments performed on the mean scalar gradient test problem with the objective of producing scalar jpdf's that remain joint-normal when started from a joint-normal initial condition. This together with  $p_0 = 1/2$  determines  $\langle Z_1 \rangle$  to be  $1/6$ . The width of the  $Z_0$  interval  $Z_{w_0}$  is chosen to be zero. This forces the particles to deterministically spend the time corresponding to  $\langle Z_0 \rangle$  in the nonmixing state. The final parameter in the age process  $Z_{w_1}$  is also chosen by numerical experimentation. Finally, the age process model parameters are:

$$p_0 = 1/2$$

$$Z_{0_t} = 1/6$$

$$Z_{0_u} = 1/6$$

$$Z_{1_t} = 0.0176$$

$$Z_{1_u} = 0.3157$$

## Discussion

### Choice of EMST as the Definition of Localness

Given a set of  $N$  points in a  $D$ -dimensional composition space, there are several definitions of proximity. Notable among them are nearest neighbor pairs, the Delaunay triangulation (DT) (and its dual the Voronoi diagram), and the MST [23]. Any of these definitions of localness can be used to define a set of edges that connect each particle to a neighbor and subsequently mixing models can be constructed based on particle-neighbor interactions that are local in composition space. It is advantageous to model these particle-neighbor interactions as pairwise-exchange models for the reasons adduced earlier in "Conservation of Means" and "Decay

of Variances.” The choice of proximity definition will depend on the model performance with respect to the list of criteria listed in “Performance Criteria for Mixing Models.” In practice, apart from the ability of the model to produce reasonable composition jpdf’s in test problems, an overriding concern is the computational expense incurred by the model.

The nearest neighbor proximity definition does not yield a satisfactory particle exchange mixing model since it collapses each nearest neighbor pair into a single composition value and the fully mixed state is never reached. In the case of the DT (or Voronoi diagram) the matrix describing the particle interaction mixing model is considerably more complex and it is difficult to predict the model behavior *a priori*. However, since the number of edges incident on a particle in the MST is a subset of the number of edges incident on the same particle in the DT, it is guaranteed that the particle interaction matrix for the DT-based mixing model will be less sparse than that for the MST-based one. The particle interaction matrix for the DT-based mixing model has no special structure and solving the corresponding evolution equation at each time step in a Monte Carlo simulation would be computationally expensive. On the other hand, the MST-based particle interaction matrix has a very special structure (owing to the underlying tree structure) that permits an  $\mathcal{O}(N)$  direct solution of the particle composition evolution equation. This alone makes the MST definition of localness attractive for the construction of mixing models that are local in composition space.

### Intermittency

The reason for introducing the intermittency feature via the age process is the formation of stranding patterns observed in the mean scalar gradient test problem. This intermittency may also be interpreted, and to some extent justified, on the following physical grounds. Regions of high scalar dissipation rate  $\chi_\phi$  ( $\chi_\phi = \Gamma \nabla \phi \cdot \nabla \phi$ , where  $\Gamma$  is the molecular diffusivity of scalar  $\phi$ ) are confined to a small fraction of the total fluid volume in physical space. Experimental evidence for large Schmidt number turbulent flows shows that 90% of the total scalar dissipation is

contained in just over 45% of the volume [25]. While the actual numerical values are very likely Reynolds number dependent, the “spottiness” in the fine structure of the scalar dissipation field is presumably characteristic of scalar mixing in high Reynolds number turbulent flows. Consequently, even though the EMST model is intended for flows with  $Sc \approx 1$ , this experimental evidence can be taken as qualitative justification for introducing the intermittency feature in the EMST model. The choices of  $p_0 = 1/2$  (the fraction of particles that participate in the mixing process being half) and the values for the residence times in states 0 and 1 for the age process have no direct support from physical evidence, but are made mainly with a view to enhancing the model performance.

### Model Properties

Since the EMST model is a pairwise-exchange model it satisfies the conservation of means, decay of variances, and boundedness principles. The EMST mixing model depends on the Euclidean norm in composition space and hence does not satisfy the independence principle. As a direct consequence, the EMST model does not satisfy the linearity principle (for equal or unequal) diffusivities either. The EMST model is invariant to rotational transformations of the set of scalars (i.e., for  $\mathbf{T}$  being an orthogonal matrix). For the homogeneous problem, even with joint-normal initial conditions, the EMST mixing model does not yield acceptable jpdf’s as shown in Fig. 4. The model exhibits a phenomenon termed “stranding” as shown in Fig. 4. The introduction of the intermittency feature was motivated by the necessity to alleviate this particular deficiency in the model. The stranding problem is alleviated by the intermittency feature, which is independent of both the number of particles per cell and the number of scalars.

The EMST model is inherently a particle model. In contrast to IEM or Curl’s model, the pdf evolution equation corresponding to the EMST model’s particle evolution equation is considerably more difficult to derive. In spite of the difficulty in mathematically analyzing the asymptotic behavior and convergence properties of the EMST model with respect to the number of particles  $N$ , numerical tests for the

mean scalar gradient test case (for two scalars and for 10 scalars), indicate that all the moments, as well as the cdf's, converge as the number of particles is increased from 512 to 8192.

The EMST model is also asymptotically local in composition space. As the number of particles per cell ( $N$ ) is increased, the characteristic edge-length (in composition space) associated with the EMST model decreases, thereby increasing localness.

The EMST model has no Reynolds number dependence and has no dependence on the small scales or the molecular diffusivity, though for equal diffusivities this can be easily introduced in the particle position evolution equation. The model assumes that the scalar dissipation is determined by the large scales which is valid in high Reynolds number turbulence. The current implementation of the model assumes equal diffusivities and has no feature to account for differential diffusion effects. Since the model is based on a one-point one-time pdf closure, it has no dependence on composition gradients or lengthscales of scalar fields. The model is currently incapable of accounting for the steepening of composition gradients due to reaction as seen in flamelet combustion.

### INERT FLOW TEST CASE

The EMST model is validated in a simple inert scalar mixing problem. One of the simplest scalar mixing problems is an inert, passive scalar decaying from specified initial conditions in decaying isotropic turbulence. Experimental studies of scalar decay in grid turbulence [13] show that the decay rate of the scalar fluctuations shows a strong dependence on the lengthscales of the initial scalar field. It is also found that there is no equilibrium value for the scalar variance decay rate. In addition there is no evidence of relaxation of the mechanical-to-scalar timescale ratio to an equilibrium value. Given that the EMST model is a closure at the level of the scalar pdf with no information of scalar gradients or scalar lengthscales, and noting that the model assumes a constant mechanical-to-scalar timescale ratio, the scalar decay

test problem does not seem appropriate for model validation.

The evolution of an inert, passive scalar field evolving in grid turbulence under an imposed linear mean scalar gradient has also been studied experimentally by Sirivat and Warhaft [5]. In this experiment the scalar field was temperature and measurements were made of the temperature variance and heat flux. This mean scalar gradient (MSG) test problem is preferable to the test case of an inert, passive scalar decaying in grid turbulence since in the MSG test the flow tends to an equilibrium where the scalar variance growth rate reaches a stationary value. Experimental evidence also shows that the ratio of mechanical-to-thermal lengthscales evolves to an equilibrium value, whereas in the decaying scalar problem this ratio does not change with time. Furthermore in the MSG test, comparison of the scalar flux values with experiment provides a test of the performance of the mixing model in conjunction with the model for particle velocity. Finally, direct numerical simulations [6] have also been performed for the MSG problem in stationary turbulence, providing additional detailed information about the scalar mixing.

A mean scalar gradient model problem is posed based on the Sirivat and Warhaft experiment [5], which is then used to test the EMST model. For a single scalar, the MSG model problem is the evolution of an inert passive scalar  $\phi_1$ , in homogeneous isotropic turbulence with an imposed linear gradient of  $\langle \phi_1 \rangle$  in the  $x_1$  direction. The velocity field in the simulation can be either decaying or stationary. For decaying turbulence the results are compared with the experimental data of Sirivat and Warhaft [5]. For the stationary case comparison with the DNS results is appropriate.

Since the EMST mixing model is intended for use in flows with multiple scalars, it is useful to study the model performance for two or more scalars. The MSG model problem extends conceptually to multiple scalars (say  $D$  in number) provided the dimension of physical space is increased to have  $D$  coordinate directions along which the mean gradients for each scalar component are imposed. In the simulation results to be presented, the mixing of two scalars is con-

sidered first and subsequently the mixing of 10 scalars.

### Moment Equations

The scalar fields can be decomposed into mean fields and fluctuating fields  $\phi_\beta = \langle \phi_\beta \rangle + \phi'_\beta$ . If the fluctuating scalar fields are initially homogeneous then they remain so for all time. The equation for the fluctuating scalar in homogeneous, isotropic turbulence with zero mean velocity can be written as

$$\begin{aligned} \frac{\partial \phi'_\beta}{\partial t} + u_j \frac{\partial \langle \phi_\beta \rangle}{\partial x_j} + \frac{\partial}{\partial x_j} (u_j \phi'_\beta - \langle u_j \phi'_\beta \rangle) \\ = \Gamma \frac{\partial^2 \phi'_\beta}{\partial x_k \partial x_k}, \end{aligned} \quad (48)$$

where  $\Gamma$  is the scalar diffusivity (assumed equal for all scalars). The scalar variance evolves as follows:

$$\frac{1}{2} \frac{\partial}{\partial t} \langle \phi'^2_\beta \rangle = -\langle \phi'_\beta u_j \rangle \frac{\partial \langle \phi_\beta \rangle}{\partial x_j} - \Gamma \left\langle \frac{\partial \phi'_\beta}{\partial x_k} \frac{\partial \phi'_\beta}{\partial x_k} \right\rangle, \quad (49)$$

with the terms on the right hand side being the production of scalar variance due to the imposed mean scalar gradient and the scalar dissipation respectively. The terms corresponding to turbulent and molecular transport are absent due to homogeneity, and the summation convention is not applied to Greek indices.

Estimates for the growth rate of the scalar variance in Eq. 49 can be obtained by simple scaling arguments. For simplicity a single scalar with mean scalar gradient in  $x_1$  is considered. Assume the scalar dissipation scales like  $\langle \phi'^2_1 \rangle / \tau_\phi$ , where  $\tau_\phi$  is the scalar timescale which to a first approximation can be assumed to be proportional to the turbulence timescale  $\tau$ . Further assuming gradient modeling for the scalar flux  $\langle \phi'_1 u_1 \rangle = \Gamma_t \partial \langle \phi_1 \rangle / \partial x_1$ , the production term scales as  $\Gamma_t (\partial \langle \phi_1 \rangle / \partial x_1)^2$ , where the eddy diffusivity  $\Gamma_t$  is assumed to scale like  $u' l$  ( $u'$  and  $l$  being the characteristic turbulence velocity and length scales respectively). If the empirical relations for the evolution of the turbulent scales in decaying isotropic grid turbulence are used ( $l \sim t^{1-n/2}$ ,  $u' \sim t^{-n/2}$ ,  $\tau \sim t$ , where  $n$  is the exponent in the velocity variance decay law for grid turbulence), then the production scales like

$(\partial \langle \phi_1 \rangle / \partial x_1)^2 t^{1-n}$  and the dissipation like  $\langle \phi'^2_1 \rangle t^{-1}$ . The growth rate of the scalar variance can become stationary if

$$\langle \phi'^2_1 \rangle \sim \left( \frac{\partial \langle \phi_1 \rangle}{\partial x_1} \right)^2 t^2 \sim t^{2-n} \approx t^{0.7}.$$

The scalar-velocity correlation coefficient is defined as

$$\rho_{\beta j} = \langle \phi'_\beta u_{(j)} \rangle / \sqrt{\langle \phi'^2_\beta \rangle \langle u'^2_{(j)} \rangle}$$

where there is no sum over bracketed indices.

The equation for the scalar flux evolution is

$$\begin{aligned} \frac{\partial}{\partial t} \langle u_i \phi'_\beta \rangle = -\langle u_i u_j \rangle \frac{\partial \langle \phi_\beta \rangle}{\partial x_j} + \langle u_j \phi'_\beta \rangle \frac{\partial \langle U_i \rangle}{\partial x_j} \\ - (\Gamma + \nu) \left\langle \frac{\partial \phi'_\beta}{\partial x_k} \frac{\partial u_i}{\partial x_k} \right\rangle \\ + \left\langle \frac{p'}{\rho} \frac{\partial \phi'_\beta}{\partial x_i} \right\rangle, \end{aligned} \quad (50)$$

where statistical homogeneity is used to simplify the dissipation and pressure-scrambling terms, and to neglect the convection and triple correlation terms. In the absence of homogeneous shear the second term on the right hand side is zero. It is customary to assume that in high Reynolds number turbulence the scalar flux dissipation can be neglected if local isotropy prevails. DNS results of Overholt and Pope [6] show that this term may not be negligible for  $R_\lambda < 350$ . For sufficiently high Reynolds number this term may be neglected and the scalar flux evolution reaches an equilibrium state when the pressure scrambling term  $\langle p' / \rho \times \partial \phi'_\beta / \partial x_k \rangle$  balances the production of scalar flux through the mean scalar gradient.

### Particle Evolution Equations

Since the velocity and fluctuating scalar fields are homogeneous, the particles in the simulation need have only velocity and scalar properties associated with them. The velocity and fluctuating scalar values are scaled as follows:

$$u_i^* = u_i / u' \quad (51)$$

$$\phi_\beta^* = \phi'_\beta / \left( \frac{u'^3}{\epsilon} \frac{\partial \langle \phi_{(\beta)} \rangle}{\partial x_{(\beta)}} \right) \quad (52)$$

TABLE 1

Values of Drift and Diffusion Coefficients in the SLM Model for Stationary and Decaying Turbulence

	Drift ( $-1/\mathcal{T}$ )	Diffusion ( $\mathcal{D}$ )
Stationary	$-3C_0/4$	$\sqrt{3C_0/2}$
Decaying	$-(1/2 + 3C_0/4)$	$\sqrt{3C_0/2}$

where  $u'$  is the standard deviation of the velocity and  $\epsilon$  is the dissipation rate of turbulence. The particles are evolved in scaled time  $s$  given by:

$$s \equiv \int_0^t \langle \omega \rangle dt, \quad (53)$$

where  $\langle \omega \rangle$  is the mean turbulent frequency.

The particle velocity evolves by the simplified Langevin model (SLM):

$$du_i^* = -\frac{1}{\mathcal{T}} u_i^* ds + \mathcal{D} dW_i, \quad (54)$$

where the drift ( $-1/\mathcal{T}$ ) and diffusion ( $\mathcal{D}$ ) coefficients are chosen appropriately for stationary or decaying turbulence. These values are given in Table 1.

The particle fluctuating compositions evolve by

$$\frac{d\phi_\beta^*}{ds} = \Theta - \frac{3}{2} u_\beta^*, \quad (55)$$

where  $\Theta$  represents the mixing model, and the second term in  $u_\beta^*$  represents the effect of the mean scalar gradient.

## EMST Model Results

### Decaying Turbulence

The EMST model is applied to the MSG model problem with two scalars. There is an imposed linear gradient of  $\langle \phi_1 \rangle$  in the  $x_1$  direction and of  $\langle \phi_2 \rangle$  in the  $x_2$  direction respectively. The velocity field is chosen to be decaying isotropic turbulence. The simulations are performed with  $N = 8192$  particles in the ensemble, initially jointly normally distributed in velocity–composition space. All the velocities and scalars have zero mean. The velocity–composition covariance matrix is diagonal. The velocity variances are all

unity, and the scalar variances are set to  $10^{-12}$ . The particle properties are incremented over time steps of  $\Delta s = 0.005$ . Scalar–velocity correlations attain nonzero stationary values for the velocity components along which the scalar has a mean gradient. The scaled scalar variances and nonzero scalar–velocity correlations evolve to their stationary values. Stationary values for all the moments are determined by time averaging. The time averaging commences when the ratio of scalar variance production to scalar dissipation reaches 92% of its stationary value which is unity. The stationary values of the mean and skewness are shown in Table 2. The evolution of the cumulative distribution function (cdf) of scalar 2 is shown in Fig. 7. The other scalar is statistically identical.

### Experimental Data

Sirivat and Warhaft [5] performed experiments to study the evolution of temperature variance and heat flux under the influence of a passive cross-stream temperature gradient in grid turbulence. The mean temperature gradient was generated using two different heating arrangements (referred to as the mandoline and the toaster). Even for this relatively simple flow it is difficult to reconcile the measurements of scalar variance growth rate and the stationary values of the scaled variance obtained by the two methods [8]. The principal reasons are: (i) uncertainty whether the toaster flow had reached a truly stationary state, (ii) uncertainty whether the Reynolds number was high enough for the measurements to be Reynolds number independent, (iii) influence of the different initial conditions in the two experiments. The EMST model predicts a stationary scaled scalar variance which lies closer to the toaster (relative error in scalar standard deviation is 16%) than the mandoline data (Table 3). The stationary scalar–velocity correlation predicted by the EMST model (relative error of 30%) is also shown in Table 3.

### Stationary Turbulence

The scaled scalar variances and nonzero scalar–velocity correlations for stationary turbulence also evolve to stationary values. The stationary values of the mean and skewness for the station-

**TABLE 2**  
 Values of the Stationary Scalar Mean and Skewness for the MSG Test Problem Using the EMST Mixing Model

	Scalar Mean	Scalar Skewness
Decaying		
Scalar 1	$-4.6 \times 10^{-10}[-1.4 \times 10^{-8}, 1.3 \times 10^{-8}]^a$	$-0.008[-0.06, 0.03]$
Scalar 2	$-3.9 \times 10^{-10}[-1.4 \times 10^{-8}, 1.2 \times 10^{-8}]$	$0.02[-0.05, 0.08]$
Stationary		
Scalar 1	$5.1 \times 10^{-10}[-1.9 \times 10^{-8}, 1.4 \times 10^{-8}]$	$-3.8 \times 10^{-2}[-8.1 \times 10^{-2}, 1.7 \times 10^{-2}]$
Scalar 2	$7.6 \times 10^{-10}[-2.2 \times 10^{-8}, 1.2 \times 10^{-8}]$	$5. \times 10^{-2}[6.5 \times 10^{-4}, 0.1]$
Stationary		
Scalar 10	$-8.5 \times 10^{-10}[-3.8 \times 10^{-9}, 2.9 \times 10^{-9}]$	$-0.22[-0.32, -0.15]$

<sup>a</sup> Corresponding minimum and maximum values in the time interval over which averaging was performed are shown in square brackets.

ary turbulence case are tabulated in Table 2. The plot of the cumulative distribution function (cdf) of scalar 2 after 10 mixing timescales is very similar to that obtained in the decaying turbulence case. DNS results of the same flow by Overholt and Pope [6] indicate a strong dependence of the scaled scalar variance on Reynolds number. The DNS results actually show a *decrease* in the scaled scalar variance with increasing Reynolds number. The DNS results also indicate that the mechanical-to-scalar timescale ratio varies from 1.8 to 3.0 and increases with Reynolds number. On the other hand in the EMST model this ratio is held constant with the choice of  $C_\phi = 2.0$ . As a consequence the model (which does not incorporate a Reynolds number dependence) is in-

capable of reproducing the range of scalar variance values obtained from the DNS. The only reasonable (and weak) conclusion that can be drawn from this comparison is that the model predictions are within the range of the DNS data. The relevant values are tabulated in Table 4.

**Multiple Scalars in Stationary Turbulence**

The EMST model is applied to the MSG model problem with 10 scalars. The numerical parameters are identical to those in the previous results. However, for this case the initial scalar variances are all chosen to be unity. Since all the scalars are statistically identical, results are presented only for the tenth scalar. The stationary values of the mean and skewness of the tenth scalar for the stationary turbulence case are

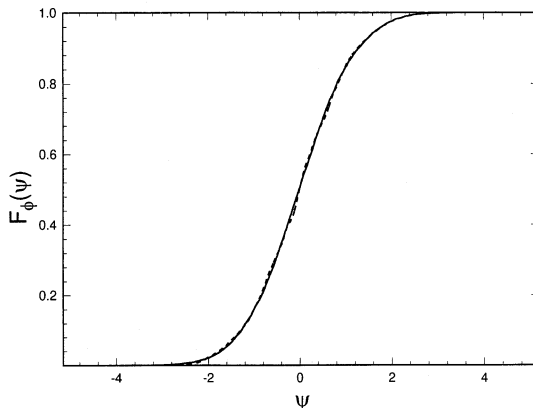


Fig. 7. Evolution of the cdf of scalar 2 in the mean scalar gradient test (decaying turbulence) using the EMST model; — initial cdf ( $s = 0$ ), - - -  $s = 5.0$ .

**TABLE 3**

Comparison of Stationary Values of the Scaled Scalar Variance and Scalar–Velocity Correlation from Experiment with the EMST Model Results for the MSG Test in Decaying Turbulence

	$\langle \phi'^2 \rangle$	$\rho$
Mandoline	1.10 [1.06, 1.18] <sup>a</sup>	-0.7
Toaster	0.75 [0.68, 0.81]	-0.68
EMST		
Model		
Scalar 1	0.53 [0.51, 0.55]	-0.48 [-0.51, -0.46]
Scalar 2	0.51 [0.49, 0.52]	-0.49 [-0.51, -0.47]

<sup>a</sup> Corresponding minimum and maximum values in the time interval over which averaging was performed are shown in square brackets.

**TABLE 4**

Comparison of Stationary Values of the Scaled Scalar Variance and Scalar-Velocity Correlation from DNS Data with the EMST Model Results for the MSG Test in Stationary Turbulence

	$\langle \phi^{*2} \rangle$	$\rho$
DNS		
$R_\lambda = 28$	1.01	-0.60
$R_\lambda = 52$	0.69	-0.56
$R_\lambda = 84$	0.59	-0.53
$R_\lambda = 185$	0.31	-0.46
EMST Model		
Scalar 1	0.62	-0.53
Scalar 2	0.60	-0.52

tabulated in Table 2. The cumulative distribution function (cdf) of the tenth scalar after 10 mixing timescales is shown in Fig. 8. While these results are not identical to those obtained from the simulation for two scalars, the departures are small enough to not invalidate the use of this model for a wide class of reactive flows. The dependence on dimensionality of the composition space arises from the variation in the structure of the EMST with dimension of the composition space, and this dependence is expected to become weaker with increasing scalar dimension.

### IEM Model Results

The evolution equation for  $\phi_\beta^*$  corresponding to the IEM model for mixing is

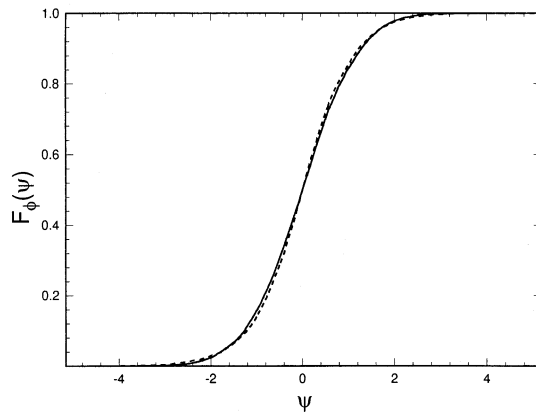


Fig. 8. Evolution of the cdf of scalar 10 after ten mixing times in the mean scalar gradient test (stationary turbulence) using the EMST model; —  $s = 0$ , - - -  $s = 5.0$ .

$$\frac{d\phi_\beta^*}{ds} = -\alpha_I \phi_\beta^* - u_\beta^* \quad (56)$$

where  $\alpha_I$  is a model constant. The relation between  $\alpha_I$  and  $C_\phi$  can be deduced from Eq. 16 to be

$$\alpha_I = \frac{C_\phi}{2}. \quad (57)$$

The corresponding scalar variance and scalar flux evolution equations are (dropping the  $\beta$  subscript since all the scalars are statistically identical)

$$\frac{d\langle u^* \phi^* \rangle}{ds} = u'^* \left( \rho_{\beta\beta} \frac{d\phi^*}{ds} + \phi^* \frac{d\rho_{\beta\beta}}{ds} \right) \quad (58)$$

$$= - \left( \alpha_I + \frac{1}{\mathcal{T}} \right) \langle u^* \phi^* \rangle - \langle u^{*2} \rangle \quad (59)$$

$$\frac{d\langle \phi^{*2} \rangle}{ds} = -\alpha_I \langle \phi^{*2} \rangle - \langle u^* \phi^* \rangle \quad (60)$$

Setting the time derivatives to zero for stationary solutions, we obtain the stationary scalar-velocity correlation and scalar variance values to be

$$\rho_{ss} = -\sqrt{\alpha_I \mathcal{T} / (1 + \alpha_I \mathcal{T})} \quad (61)$$

$$\langle \phi^{*2} \rangle_{ss} = -\frac{\rho_{ss} u'^*}{\alpha_I}. \quad (62)$$

The stationary values of the scalar-velocity correlation and scaled scalar variance for stationary and decaying turbulence cases as predicted by these formulae (using the values for the model constants given in Table 1) are tabulated in Table 5. It is seen that the IEM model predictions are closer to the experimental results for the decaying case, whereas in the stationary case the large variation with Reynolds number in the DNS results precludes any meaningful comparison.

Since the model for scalar dissipation in the scalar variance equation (Eq. 49) is the same for both the IEM and EMST models, the differences in the stationary scalar variance results must arise from the production term. This can be explained as arising from differences in the nonzero scalar flux terms  $\langle \phi'_\beta u_j \rangle$ . Recently, Pope [26] has shown that since the scalar flux is

TABLE 5

Comparison of IEM and EMST Model Predictions of Stationary Scaled Scalar Variance and Scalar-Velocity Correlation for the Mean Scalar Gradient Model Problem for Stationary and Decaying Turbulence

	IEM	EMST
Stationary		
$\langle \phi^{*2} \rangle_{ss}$	0.873	0.62
$\rho_{ss}$	-0.62	-0.53
Decaying		
$\langle \phi^{*2} \rangle_{ss}$	0.73	0.53
$\rho_{ss}$	-0.57	-0.48

independent of the diffusivity at high Peclet number, the modeled scalar flux  $\langle \phi_{\beta}^* u_j^* \rangle$  should be independent of the mixing model (i.e., it should be determined from the drift coefficients in the particle velocity model). The IEM model as described in this paper has a spurious source term in the modeled scalar flux equation. A correction to this model has also been suggested by Pope [26] but numerical implementation of this may not be straightforward. It should be noted that the EMST model also violates the diffusivity independence principle as expressed in terms of the modeled scalar flux equation's independence of the mixing model coefficients. Any two mixing models that satisfy the diffusivity independence principle would yield identical results for the stationary scaled variance (in the MSG model problem) and scalar-velocity correlation, provided the same velocity model was used. Of course there would be differences in the scalar cdf's which would also be manifest in the higher scalar moments.

## DIFFUSION FLAME TEST RESULT

The EMST mixing model is applied to the diffusion flame test which is an idealized reactive flow test problem. The objective is to verify the hypothesis that a mixing model that is local in composition space will yield the correct physical behavior for this particular test case. To recapitulate, consider an idealized diffusion flame in homogeneous isotropic turbulence with infinitely fast chemistry. The fluid composition is represented by two variables: mixture fraction  $\xi$  and a reaction progress variable  $Y$ . The initial condition ( $t = 0$ ) for mixture fraction is chosen

to be a  $\beta$ -distribution with mean and variance which correspond to a typical experiment. The progress variable is initially at equilibrium (denoted  $Y_e$ ). The one-step, irreversible reaction is confined to a region in composition space as shown in Fig. 1.

As the flow evolves from this homogeneous initial condition, reactants enter the reaction zone by mixing and are instantly reacted to form products resulting in flame sheet combustion [3]. Since the reaction is infinitely fast compared to the mixing and is also irreversible, the only stable solution for  $t > 0$  corresponds to complete combustion, i.e., all the particles lie on the equilibrium line.

The evolution of the composition jpdf is computed using a Monte Carlo particle method where the discrete jpdf of composition, which is an ensemble of delta functions in the two-dimensional composition space, is represented by an ensemble of 4096 particles with two properties: mixture fraction  $\xi$  and progress variable  $Y$ . At any time  $t$  in the simulation, particle properties are advanced over a time step  $\Delta t$  which is chosen to be a user-defined fraction ( $4 \times 10^{-3}$  for the diffusion flame test) of the minimum physical timescale in the problem. For the diffusion flame test with infinitely fast chemistry the chemical time scale is zero. Consequently the minimum physical timescale is the only other timescale in the problem, which is the mixing timescale  $\tau_\phi$ . Both mixture fraction and progress variable properties of the particles are advanced using the EMST mixing model. The effect of infinitely fast, irreversible reaction is accounted for by setting  $Y$  to the corresponding equilibrium value. The scatter plot in composition space at time  $t = 0.8\tau_\phi$  (Fig. 9) shows that the EMST model reproduces the expected physical behavior. It should be noted, however, that localness is affected by the number of particles  $N_T$  which are used to form the EMST.

The same simulation is performed with the IEM mixing model, and the corresponding scatter plot in composition space at time  $t = 0.8\tau_\phi$  is shown in Fig. 10. It is clear that particles do not all lie on the equilibrium line and the model fails to reproduce the expected physical behavior. Particles corresponding to composition values outside the reaction zone relax to the mean composition and are drawn away from their

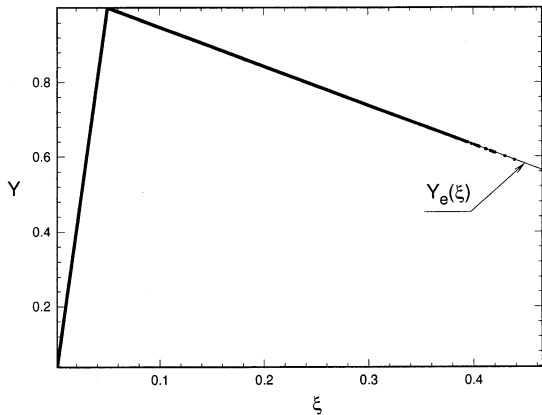


Fig. 9. Scatter plot of reaction progress variable  $Y$  vs.  $\xi$ : EMST model result for the diffusion flame test at  $t = 0.8\tau_{\phi}$ .

initial condition on the equilibrium line. Particles in the reaction zone are of course instantly reacted back to their equilibrium values at each time step. This accounts for the piecewise linear scatter plot in Fig. 10 [7].

## CONCLUSION

A new model for the mixing of multiple reactive scalars has been developed. This pairwise exchange model is based on Euclidean minimum spanning trees constructed in composition space and possesses the important property that it is local in composition space. It also satisfies the mean conservation and variance decay properties. Boundedness of compositions is preserved by the EMST model. However, this

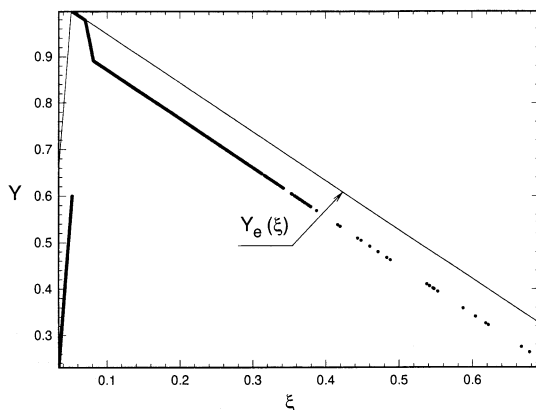


Fig. 10. Scatter plot of reaction progress variable  $Y$  vs.  $\xi$ : IEM model result for the diffusion flame test at  $t = 0.8\tau_{\phi}$ .

model does not satisfy the independence and linearity properties.

The model is applied to an inert scalar mixing test problem based on the imposed mean temperature gradient experiment of Sirivat and Warhaft [5]. Reasonable results are obtained for the scalar variance and scalar-velocity correlation but the agreement with experimental data (which has a high variability depending on the heater configuration used) is not close. The model results are also compared with the DNS data of Overholt and Pope [6] for a similar mean scalar gradient problem in stationary turbulence. Unfortunately the comparison is not conclusive since there is a strong Reynolds number dependence in the DNS results, whereas the model incorporates no Reynolds number dependence. It is assumed in the modeling that the Reynolds number is very large.

Finally the model is tested in a reactive flow test problem called the diffusion flame test. Excellent results are obtained using the EMST model, confirming the hypothesis that the localness principle forms a sound basis for reproducing the expected physical behavior in this problem. These are contrasted with the incorrect results obtained using the IEM model. Similar deficiencies have been documented with Curl's model also [3].

The EMST model has been applied to piloted jet diffusion flames and preliminary qualitative results are encouraging [7]. Further quantitative results are anticipated and will provide a further test for the model. The model is also currently being applied to a variety of reactive flow test problems which will provide detailed information concerning the model behavior in various flow situations.

*This work was supported by the Air Force Office of Scientific Research, Grant F49620-94-1-0098.*

## REFERENCES

1. Pope, S. B., *Prog. Energy Combust. Science* 11:119-192 (1985).
2. Norris, A. T., and Pope, S. B., *Combust. Flame* 100: 211-220 (1995).
3. Norris, A. T., and Pope, S. B., *Combust. Flame* 83: 27-42 (1991).
4. Dopazo, C., *Phys. Fluids* 18:397-404 (1975).

5. Sirivat, A., and Warhaft, Z., *J. Fluid Mech.* 128:323–346 (1983).
6. Overholt, M. R., and Pope, S. B., *Phys. Fluids* 8(11): 3128–3148 (1996).
7. Masri, A. R., Subramaniam, S., and Pope, S. B., In *Twenty-Sixth Symposium (International) on Combustion*, The Combustion Institute, Pittsburgh, 1996.
8. Subramaniam, S., (1997). Ph.D. thesis, Cornell University.
9. Golub, G. E., and Van Loan, C. F., *Matrix Computations*, 2nd ed., Johns Hopkins, Baltimore, MD 1989.
10. Pope, S. B., *Phys. Fluids* 26:404–408 (1983).
11. Jayesh and Warhaft, Z., *Phys. Fluids A* 4(10):2292–2307 (1992).
12. Eswaran, V., and Pope, S. B., *Phys. Fluids* 31(3):506–520 (1988).
13. Warhaft, Z., and Lumley, J. L., *J. Fluid Mech.* 88:659–684 (1978).
14. Juneja, A., and Pope, S. B., *Phys. Fluids* 8:2161–2184 (1996).
15. Curl, R. L., *A.I.Ch.E.J.* 9(175) (1963).
16. Pope, S. B., *Combust. Sci. Technol.* 28:131–145 (1982).
17. Valiño, L., and Dopazo, C., *Phys. Fluids A* 3(12):3034–3037 (1991).
18. Fox, R. O., *Phys. Fluids A* 4(6):1230–1244 (1992).
19. Chen, H., Chen, S., and Kraichnan, R. H., *Phys. Rev. Lett.* 63(24):2657–2660 (1989).
20. Pope, S. B., *Theoret. Computa. Fluid Dynamics* 2(5/6): 255–270 (1991).
21. Resnick, S. I., *Adventures in Stochastic Processes*, Birkhäuser, Boston, MA 1992.
22. Aho, A. V., Hopcroft, J. E., and Ullman, J. D., *Data Structures and Algorithms*, Addison-Wesley, Reading, MA, 1983.
23. Preparata, F. P., and Shamos, M. I., *Computational Geometry: An Introduction*, Springer-Verlag, New York, 1985.
24. Deo, N., *Graph Theory with Applications to Engineering and Computer Science*, Prentice-Hall, Englewood Cliffs, New Jersey, 1974.
25. Dahm, W. J. A., Southerland, B. K., and Buch, K. A., *Phys. Fluids A* 3(5):1115–1127 (1991).
26. Pope, S. B., *J. Fluid Mech.* 359:299–312 (1998).

Received 1 April 1997; accepted 13 February 1998